



**NIST Technical Note  
NIST TN 2232**

**Oxygen-Limited Fires Inside  
Under-Ventilated Enclosures  
(OLIVE-FIRE)**

Kevin McGrattan  
Isaac Leventon

This publication is available free of charge from:  
<https://doi.org/10.6028/NIST.TN.2232>

**NIST Technical Note  
NIST TN 2232**

**Oxygen-Limited Fires Inside  
Under-Ventilated Enclosures  
(OLIVE-FIRE)**

Kevin McGrattan  
Isaac Leventon  
*Fire Research Division  
Engineering Laboratory*

This publication is available free of charge from:  
<https://doi.org/10.6028/NIST.TN.2232>

August 2022



U.S. Department of Commerce  
*Gina M. Raimondo, Secretary*

National Institute of Standards and Technology  
*Laurie E. Locascio, NIST Director and Under Secretary of Commerce for Standards and Technology*

Certain commercial entities, equipment, or materials may be identified in this document in order to describe an experimental procedure or concept adequately. Such identification is not intended to imply recommendation or endorsement by the National Institute of Standards and Technology, nor is it intended to imply that the entities, materials, or equipment are necessarily the best available for the purpose.

**NIST Technical Series Policies**

[Copyright, Fair Use, and Licensing Statements](#)

[NIST Technical Series Publication Identifier Syntax](#)

**Publication History**

Approved by the NIST Editorial Review Board on 2022-08-04

**How to cite this NIST Technical Series Publication:**

K. McGrattan, I. Leventon, (2022) Oxygen-Limited Fires Inside Under-Ventilated Enclosures (OLIVE-FIRE). (National Institute of Standards and Technology, Gaithersburg, MD), NIST TN 2232. <https://doi.org/10.6028/NIST.TN.2232>

**NIST Author ORCID iDs**

Kevin McGrattan: 0000-0002-1135-1274

Isaac Leventon: 0000-0002-8835-8087

**Contact Information**

[kevin.mcgrattan@nist.gov](mailto:kevin.mcgrattan@nist.gov)

## **Abstract**

This report documents a series of fire experiments performed within steel electrical enclosures. The objective is to validate a simple empirical model that predicts the maximum heat release rate of a fire within a closed compartment as a function of its ventilation openings. Based on these experiments, the relative standard uncertainty in model prediction is shown to be 25 % owing largely to the uncertainty in the leakage area of the enclosure.

## **Keywords**

Electrical enclosures; Under-ventilated fire.

## Table of Contents

1. Introduction . . . . .	1
1.1. Background . . . . .	1
1.2. A Simple Enclosure Fire Model . . . . .	1
2. Description of Experiments . . . . .	3
2.1. Description of the Electrical Enclosures . . . . .	3
2.2. Determining Enclosure Vent and Leakage Areas . . . . .	8
3. Experimental Results . . . . .	12
4. Estimation of Maximum Heat Release Rate . . . . .	15
4.1. Model Parameters . . . . .	15
4.2. Applying the Model . . . . .	19
5. Conclusion . . . . .	20
6. References . . . . .	21
A. Model Derivation . . . . .	22
B. Enclosure Drawings . . . . .	23
C. Summary of Experiments . . . . .	30
C.1. Experiment 1 . . . . .	31
C.2. Experiment 2 . . . . .	32
C.3. Experiment 3 . . . . .	33
C.4. Experiment 4 . . . . .	34
C.5. Experiment 5 . . . . .	35
C.6. Experiment 6 . . . . .	36
C.7. Experiment 7 . . . . .	37
C.8. Experiment 8 . . . . .	38
C.9. Experiment 9 . . . . .	39
C.10. Experiment 10 . . . . .	40
C.11. Experiment 11 . . . . .	41
C.12. Experiment 12 . . . . .	42
C.13. Experiment 13 . . . . .	43
C.14. Experiment 14 . . . . .	44
C.15. Experiment 15 . . . . .	45

C.16. Experiment 16 . . . . .	46
C.17. Experiment 17 . . . . .	47
C.18. Experiment 18 . . . . .	48
C.19. Experiment 19 . . . . .	49
C.20. Experiment 20 . . . . .	50
C.21. Experiment 21 . . . . .	51
C.22. Experiment 22 . . . . .	52
C.23. Experiment 23 . . . . .	53
C.24. Experiment 24 . . . . .	54
C.25. Experiment 25 . . . . .	55
C.26. Experiment 26 . . . . .	56
C.27. Experiment 27 . . . . .	57
C.28. Experiment 28 . . . . .	58
C.29. Experiment 29 . . . . .	59
C.30. Experiment 30 . . . . .	60
C.31. Experiment 31 . . . . .	61
C.32. Experiment 32 . . . . .	62

## List of Tables

Table 1. Enclosure description and approximate dimensions . . . . .	3
Table 2. Enclosure vent and leakage areas. The relative standard uncertainty of the leakage area is 5 %. . . . .	9
Table 3. Summary of experimental results . . . . .	13

## List of Figures

Fig. 1. Photographs of Enclosures #1 and #2 . . . . .	4
Fig. 2. Photographs of Enclosures #3 and #4 . . . . .	5
Fig. 3. Photographs of Enclosures #5 and #6 . . . . .	6
Fig. 4. Photographs of Enclosures #7 and #8 . . . . .	7
Fig. 5. Leakage measurement for Enclosure #6 . . . . .	10
Fig. 6. Results of enclosure leakage measurements . . . . .	11
Fig. 7. Comparison of predicted versus measured maximum heat release rate . . . . .	14
Fig. 8. Photograph of flames escaping though a seam . . . . .	15
Fig. 9. Photograph of large outdoor electrical enclosure. . . . .	18
Fig. 10. Louvers and miscellaneous leakage paths (yellow lines). . . . .	18

Fig. 11. Sketch of Enclosure #1 and #2. . . . .	23
Fig. 12. Sketch of Enclosure #3. . . . .	24
Fig. 13. Sketch of Enclosure #4. . . . .	25
Fig. 14. Sketch of Enclosure #5. . . . .	26
Fig. 15. Sketch of Enclosure #6. . . . .	27
Fig. 16. Sketch of Enclosure #7. . . . .	28
Fig. 17. Sketch of Enclosure #8. . . . .	29
Fig. 18. Heat release rate, gas concentrations, and photograph of Experiment 1. . .	31
Fig. 19. Heat release rate, gas concentrations, and photograph of Experiment 2. . .	32
Fig. 20. Heat release rate, gas concentrations, and photograph of Experiment 3. . .	33
Fig. 21. Heat release rate, gas concentrations, and photograph of Experiment 4. . .	34
Fig. 22. Heat release rate, gas concentrations, and photograph of Experiment 5. . .	35
Fig. 23. Heat release rate, gas concentrations, and photograph of Experiment 6. . .	36
Fig. 24. Heat release rate, gas concentrations, and photograph of Experiment 7. . .	37
Fig. 25. Heat release rate, gas concentrations, and photograph of Experiment 8. . .	38
Fig. 26. Heat release rate, gas concentrations, and photograph of Experiment 9. . .	39
Fig. 27. Heat release rate, gas concentrations, and photograph of Experiment 10. . .	40
Fig. 28. Heat release rate, gas concentrations, and photograph of Experiment 11. . .	41
Fig. 29. Heat release rate, gas concentrations, and photograph of Experiment 12. . .	42
Fig. 30. Heat release rate, gas concentrations, and photograph of Experiment 13. . .	43
Fig. 31. Heat release rate, gas concentrations, and photograph of Experiment 14. . .	44
Fig. 32. Heat release rate, gas concentrations, and photograph of Experiment 15. . .	45
Fig. 33. Heat release rate, gas concentrations, and photograph of Experiment 16. . .	46
Fig. 34. Heat release rate, gas concentrations, and photograph of Experiment 17. . .	47
Fig. 35. Heat release rate, gas concentrations, and photograph of Experiment 18. . .	48
Fig. 36. Heat release rate, gas concentrations, and photograph of Experiment 19. . .	49
Fig. 37. Heat release rate, gas concentrations, and photograph of Experiment 20. . .	50
Fig. 38. Heat release rate, gas concentrations, and photograph of Experiment 21. . .	51
Fig. 39. Heat release rate, gas concentrations, and photograph of Experiment 22. . .	52
Fig. 40. Heat release rate, gas concentrations, and photograph of Experiment 23. . .	53
Fig. 41. Heat release rate, gas concentrations, and photograph of Experiment 24. . .	54
Fig. 42. Heat release rate, gas concentrations, and photograph of Experiment 25. . .	55
Fig. 43. Heat release rate, gas concentrations, and photograph of Experiment 26. . .	56
Fig. 44. Heat release rate, gas concentrations, and photograph of Experiment 27. . .	57
Fig. 45. Heat release rate, gas concentrations, and photograph of Experiment 28. . .	58
Fig. 46. Heat release rate, gas concentrations, and photograph of Experiment 29. . .	59
Fig. 47. Heat release rate, gas concentrations, and photograph of Experiment 30. . .	60
Fig. 48. Heat release rate, gas concentrations, and photograph of Experiment 31. . .	61
Fig. 49. Heat release rate, gas concentrations, and photograph of Experiment 32. . .	62

## 1. Introduction

Electrical enclosures housing equipment such as circuit breakers, motor controls centers, etc., are a common source of fire in industrial settings, and the heat release rate (HRR) of these fires is an important consideration in probabilistic risk assessments. The HRR of fires in relatively open, well-ventilated enclosures is controlled largely by the quantity and flammability of the contents, but for enclosures with limited ventilation, the HRR is controlled largely by the supply of air. To date, there is limited experimental data to quantify the HRR in closed, electrical enclosures; thus, the experiments described in this report are aimed at validating a simple empirical model that predicts the maximum HRR of fires in closed steel enclosures.

### 1.1. Background

In 2005, the U.S. Nuclear Regulatory Commission (NRC) and the Electric Power Research Institute (EPRI) jointly published guidance for performing probabilistic risk assessments (PRA) for nuclear power plants [1]. Statistical distributions are given for the peak HRR for five categories of electrical enclosures based on the amount of electrical wiring and cables, their IEEE 383 [2] qualification status, and the amount of ventilation. This classification system was developed using data from fire experiments performed at Sandia National Laboratories (SNL) [3] and the Finnish laboratory VTT [4–6]. While the guidance represented the state of knowledge at the time it was published, its use in practice has raised issues that are not addressed in the original guidance document.

The Heat Release Rates of Electrical Enclosure Fires (HELEN-FIRE) program [7] was initiated in 2014 as part of an effort to address the lack of experimental data. A total of 112 full-scale experiments were conducted to measure the HRR of fires in a variety of electrical enclosures typically found in nuclear plants. Using data from the HELEN-FIRE and other test programs, a new classification system was developed [8] that characterizes enclosures based on their function, volume, combustible content, and ventilation. The classification of enclosures by volume is easily done by external visual inspection. Large and medium volumes can be further sub-divided according to combustible load, cable materials, and ventilation so that the expected peak HRR values can be estimated using visual inspection only.

For various reasons, it is difficult to visually inspect the interior of an electrical enclosure in an operating plant; thus, it would be useful to develop a simple method to estimate the maximum possible HRR for a closed enclosure without the need to open it. The experiments described in this report provide data to validate one such method.

### 1.2. A Simple Enclosure Fire Model

Mangs and Keski-Rahkonen of VTT Building Technology in Finland [4] developed an empirical model that predicts the maximum heat release rate of a fire within a closed steel

electrical enclosure with relatively small ventilation openings of area  $A_i$  (inlet) and  $A_e$  (exhaust) separated by a vertical distance  $H$ . The model is based on the estimate of the mass flow of air through the enclosure (see Appendix A for a derivation):

$$\dot{m} = C\rho_0\sqrt{2gH}\sqrt{\frac{1 - 1/\tau}{1/A_i^2 + \tau/A_e^2}} \quad ; \quad \tau = \frac{T}{T_0} \quad (1)$$

where  $C$  is the discharge coefficient of the vents,  $\rho_0$  is the density of ambient air,  $g$  is the acceleration of gravity, and  $T$  is the (absolute) temperature inside the enclosure and  $T_0$  outside. The maximum heat release rate of a fire within the enclosure is estimated to be

$$\dot{Q}_{\max} = \chi \dot{m} \Delta h_{\text{air}} \quad (2)$$

where  $\chi$  is the fraction of the oxygen drawn into the enclosure that is actually consumed by the fire and  $\Delta h_{\text{air}} \approx 3000$  kJ/kg is the energy released per unit mass of air consumed in the combustion process. Mangs and Keski-Rahkonen [4] take  $\chi$  to be approximately 0.5; that is, about half of the oxygen in the air drawn into the enclosure is consumed by the fire. The rest exits through the exhaust vent.

This advantage of this model is that it only requires information about the size and relative location of the inlet and exhaust vents, but not the nature of the contents. This is important because in operating plants it is usually not possible to open the enclosures for safety reasons.

The objective of the experiments described below is to validate this empirical model.

## 2. Description of Experiments

Eight electrical enclosures were shipped to the National Fire Research Laboratory (NFRL) at NIST in November, 2021. These enclosures were originally installed at a sewage treatment plant in Pennsylvania, but much of their interior equipment had been removed.

### 2.1. Description of the Electrical Enclosures

Photographs of the enclosures are shown in Figs. 1 through 4, and exterior sketches are shown in Appendix B. The nominal dimensions of the enclosures are listed in Table 1. Some of the enclosures have ventilation panels near the top and bottom, and all have seams and small openings to accommodate wiring, bus bars, door panels, and so on.

**Table 1.** Enclosure description and approximate dimensions

No.	Type	Width		Depth		Height		Volume	
		(m)	(in)	(m)	(in)	(m)	(in)	(m <sup>3</sup> )	(ft <sup>3</sup> )
1	Switchgear	1.68	66	1.52	60	2.31	91	5.90	208
2	Switchgear	1.68	66	1.52	60	2.31	91	5.90	208
3	Motor Control Center	0.91	36	1.40	55	2.34	92	2.98	105
4	Switchgear	0.97	38	1.56	62	2.36	93	3.57	126
5	Motor Control Center	1.83	72	1.37	54	2.32	92	5.82	206
6	Motor Control Center	0.51	20	0.36	14	2.29	90	0.42	15
7	Switchgear	2.49	98	1.02	40	2.39	94	6.07	214
8	Motor Control Center	1.52	60	0.51	20	2.32	92	1.80	64

The different panels and doors varied from 16 gauge steel (nominally 0.0595 in or approximately 1.5 mm) to 11 gauge steel (nominally 0.12 in or approximately 3.0 mm).



**Fig. 1.** Photographs of Enclosures #1 and #2. The exteriors of each are identical. At right in the top photograph is the natural gas burner. The exterior wiring is for thermocouples.



**Fig. 2.** Photographs of Enclosures #3 (top) and #4 (bottom). The steel plates in the top photograph have replaced control panels and are sealed with heat-resistant caulk. The hose leading to the top is an *ad hoc* sprinkler system. The circular window in the bottom photograph is a view port that was added to ensure that the fire did not extinguish.



**Fig. 3.** Photographs of Enclosures #5 (top) and #6 (bottom). Steel plates sealed with heat-resistant caulk replace control panels.



**Fig. 4.** Photographs of Enclosures #7 (top) and #8 (bottom). The acrylic windows in the top photograph were lined with aluminum tape to prevent their rubber gaskets from melting.

## 2.2. Determining Enclosure Vent and Leakage Areas

All of the enclosures have various amounts of leakage depending on their function and construction. The total area of both leaks and vents,  $A_t$ , can be measured by pumping air into the enclosure at a known volume flow rate,  $\dot{V}$ , while measuring the pressure difference between the inside and outside,  $\Delta p$ . The device<sup>1</sup> shown in Fig. 5 was designed to measure the leakage of residential ventilation ducts, but it was easily adapted to measure the leakage of the steel enclosures. After making measurements for all eight enclosures, it was found that the following equation best fit the data:

$$\dot{V} = CA_t \left( \frac{2\Delta p}{\rho_0} \right)^{0.5} \left( \frac{\Delta p}{\Delta p_{\text{ref}}} \right)^{0.1} \quad (3)$$

Typically, the volume flow rate,  $\dot{V}$ , is expressed in units of  $\text{m}^3/\text{s}$ , the area,  $A_t$ , in  $\text{m}^2$ , the pressure difference,  $\Delta p$ , in Pa, and the ambient density,  $\rho_0 \approx 1.2 \text{ kg}/\text{m}^3$ . The discharge coefficient,  $C = 0.61$ , is appropriate for sharp-edged orifice plates and is recommended by the manufacturer for leakage measurements. The extra factor in the expression represents a weak relationship between the discharge coefficient and the pressure rise. The reference pressure,  $\Delta p_{\text{ref}}$ , is taken as 1 Pa to maintain unit consistency. The results of the enclosure leakage measurements are displayed in Fig. 6.

Table 2 lists the leakage area, vent area, and total area for the eight enclosures. In most cases, the actual vents were sealed during the leakage measurement; thus, the “Leakage Area” was obtained directly from Eq. (3) while the “Vent Area” was either directly measured, or it was obtained by uncovering some of the vent openings and repeating the pressure measurement. For Enclosure #2, it was possible to measure the actual vent openings with a ruler and then check this direct measurement with that inferred from Eq. (3). The two values were within 5 % (relative standard uncertainty), the uncertainty estimate given by the manufacturer.

---

<sup>1</sup>Model DL1-DM4 Duct Leakage Testing System manufactured by Infiltec Inc. of Falls Church, Virginia

**Table 2.** Enclosure vent and leakage areas. The relative standard uncertainty of the leakage area is 5 %.

No.	Leakage Area		Seam Length		Seam Width		Vent Area		Total Area	
	(m <sup>2</sup> )	(in <sup>2</sup> )	(m)	(in)	(mm)	(in)	(m <sup>2</sup> )	(in <sup>2</sup> )	(m <sup>2</sup> )	(in <sup>2</sup> )
1	0.109	171	45	1764	2.5	0.097	0.164	254	0.274	425
2	0.172	264	45	1764	3.8	0.149	0.164	254	0.334	518
3	0.039	60	42	1640	0.9	0.037	0.032	50	0.071	110
4	0.044	67	37	1464	1.2	0.046	0.030	47	0.073	113
5	0.060	93	68	2676	0.9	0.035	0.108	167	0.168	260
6	0.017	26	21	830	0.8	0.032	0.000	0	0.017	26
7	0.022	34	65	2542	0.3	0.013	0.039	61	0.061	95
8	0.078	122	43	1712	1.8	0.072	0.000	0	0.079	122



**Fig. 5.** Leakage measurement for Enclosure #6 using the DM4 Dual Digital Micro-Manometer manufactured by Infiltec Inc., Falls Church, Virginia.

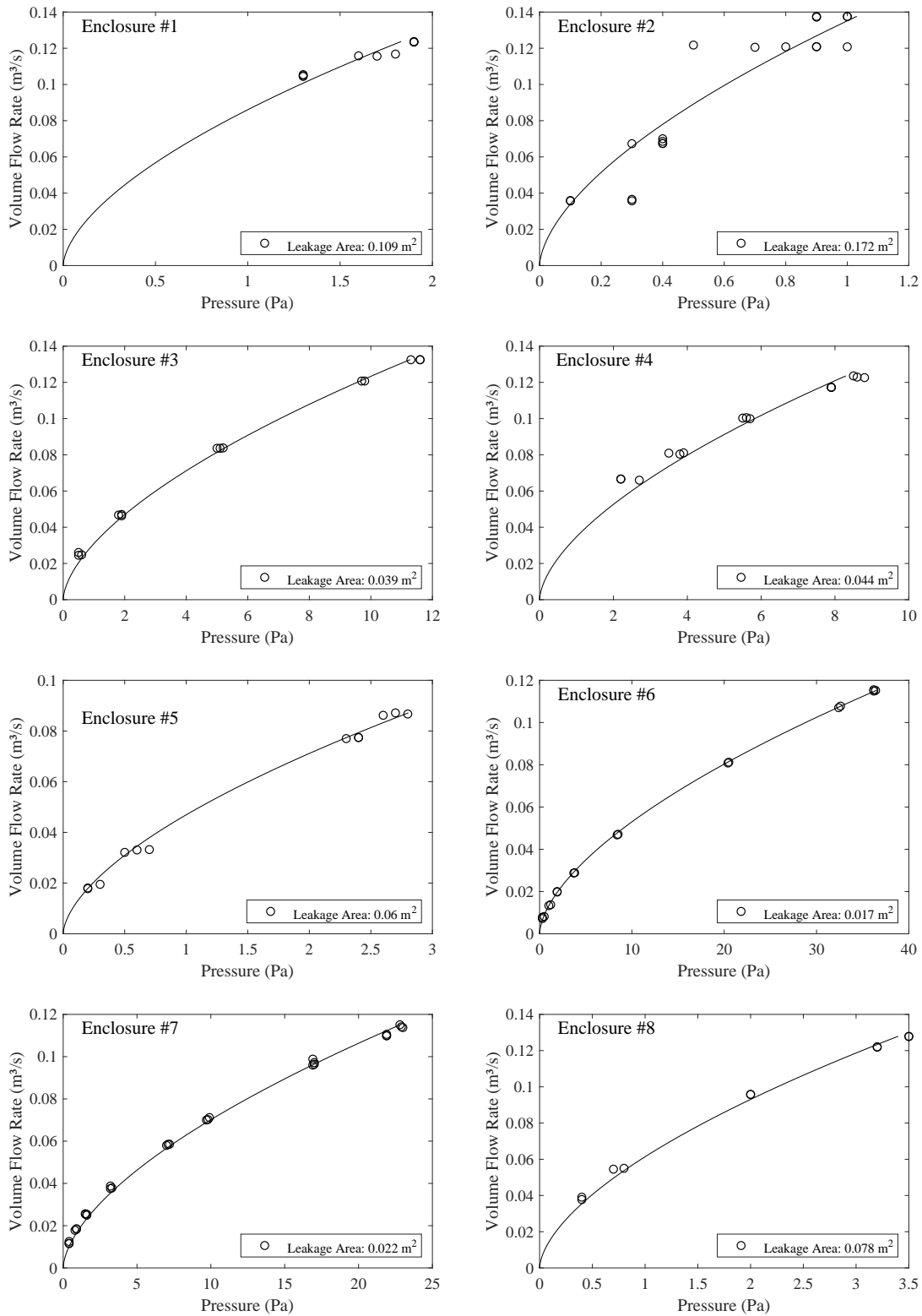


**Fig. 6.** Results of enclosure leakage experiments. Note that the scatter decreases as the range of pressure increases.

### 3. Experimental Results

In February and March of 2022, 32 full-scale fire experiments were conducted in the National Fire Research Laboratory at NIST. Two types of experiments were conducted. The first type made use of a natural gas burner. For the motor control centers, Enclosures #6 and #8, a small sand burner of approximate dimension 18 cm (7 in) by 18 cm was placed within one of the lower compartments, as shown in Fig. 36. For the other enclosures, a 30 cm (12 in) by 30 cm by 50 cm (20 in) tall burner was set on the floor. The surface of the burner was lined with approximately 2.5 cm (1 in) thick ceramic fiber insulation. A photograph of this burner is shown in Fig. 1.

In the experiments that used a gas burner, the HRR was ramped up in increments of approximately 50 kW, typically, until the fire became under-ventilated; that is, until the HRR measured using oxygen consumption calorimetry no longer matched the value expected of the given fuel flow rate. Thus, the theoretical and actual HRR were monitored until the two diverged, indicating that the maximum HRR had been reached.

The second type of experiment made use of a variety of plastics or a single type of electrical cable. Ignition was achieved using a natural gas line burner that generated approximately 25 kW. The electrical cable had a diameter of approximately 1.5 cm (0.6 in), with seven PE-insulated 12 AWG conductors and a PVC jacket<sup>2</sup>. The plastics were cut from sheets that were typically 6 mm (0.25 in) thick. Both the cable and the plastics were chosen specifically because each could sustain a relatively large fire with a maximum HRR outside of the enclosure that was significantly higher than the enclosure's theoretical maximum.

The enclosures were instrumented with sheathed thermocouples and a single extractive sampling probe measuring O<sub>2</sub>, CO<sub>2</sub>, and CO. The thermocouples were typically installed on two sides of the enclosure at distances of approximately 0.3 m (1 ft), 0.9 m (3 ft) and 1.8 m (6 ft) from the ceiling. The oxygen probe was located approximately 0.3 m (1 ft) from the ceiling.

The results of the 32 experiments are summarized in Table 3, and each experiment is briefly described in Appendix C. The method for estimating the maximum heat release rate for each experiment is outlined in Section 4. Figure 7 displays a comparison of the maximum heat release rate predicted by the empirical model and that measured in the experiments.

The empirical model of the maximum HRR, Eqs. (1) and (2), under-predicts the measured maximum HRR by approximately 4 %, and the standard deviation of the relative differences is approximately 0.25. The parameters that contribute the most to the scatter are the combustion efficiency,  $\chi$ ; the vent and leakage areas,  $A_i$ ,  $A_e$ ,  $A_l$ ; the height,  $H$ ; and the discharge coefficient,  $C$ . Of these, the leakage area,  $A_l$ , is most likely the greatest source of uncertainty because it is not possible to measure it during a fire. As seen in the photograph shown in Fig. 8, steel plates that form the external skin of the enclosure expand upon heat-

---

<sup>2</sup>The cable is referred to as #900 in Ref. [9]

**Table 3.** Summary of experimental results. The plus sign added to the Leak Area of Experiments 1 and 2 indicate that the gaps between steel panels opened substantially during the experiment due to heating. The column labelled “Height” refers to the distance between the inlet and exhaust vents,  $H$ , not the actual height of the enclosure.

Exp. No.	Encl. No.	Fuel Type	Leak Area (m <sup>2</sup> )	Vent Area (m <sup>2</sup> )	Height (m)	Max HRR (kW, model)	Max HRR (kW, meas.)
1	5	NG	0.060+	0.108	2.1	289	540
2	5	NG	0.060+	0.108	2.1	289	400
3	5	NG	0.060	0.032	1.1	115	160
4	5	NG	0.060	0	1.5	87	105
5	5	NG	0.060	0	1.5	87	105
6	5	Plastics	0.060	0.032	1.1	115	90
7	5	Plastics	0.060	0.108	2.1	289	270
8	5	NG	0.060	0.108	2.1	289	230
9	6	NG	0.017	0	1.4	24	45
10	6	Cable	Open	Open	N/A	N/A	40
11	6	Cable	0.017	0	1.4	24	25
12	2	NG	0.172	0.164	1.8	534	580
13	2	NG	0.172	0	1.5	248	270
14	2	Plastics	0.172	0	1.5	248	180
15	3	NG	0.039	0	1.5	57	70
16	3	NG	0.039	0.016	2.1	95	100
17	3	NG	0.039	0.032	2.1	123	130
18	3	Plastics	0.039	0.032	2.1	123	90
19	8	NG	0.078	0	1.5	115	165
20	8	Cable	0.078	0	1.5	115	120
21	8	Cable	0.078	0	1.5	115	85
22	7	NG	0.022	0.022	2.0	74	65
23	7	NG	0.022	0.019	2.0	69	60
24	7	NG	0.022	0.045	2.0	111	180
25	7	Plastics	0.022	0.045	2.0	111	170
26	4	NG	0.044	0.030	1.8	117	120
27	4	NG	0.044	0.030	1.8	117	125
28	4	Plastics	0.044	0.030	1.8	117	80
29	1	NG	0.109	0	1.5	160	240
30	1	NG	0.109	0.070	2.0	207	250
31	1	NG	0.109	0.070	2.0	295	400
32	1	Plastics	0.109	0	1.5	160	170

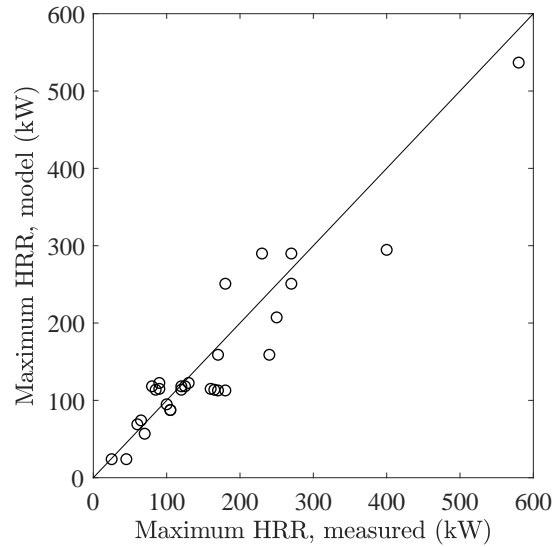


**Fig. 7.** Comparison of predicted versus measured maximum heat release rate.

ing and open up sizeable gaps. For Experiments 1 and 2, these gaps were so large that the results of these two experiments could not be used in the final summary plot because there was no way to estimate the leakage area. For all subsequent experiments, the steel panels were reinforced with extra screws to prevent excessive buckling.



Fig. 8. Photograph showing flames emerging from a seam.

#### 4. Estimation of Maximum Heat Release Rate

The modeled maximum heat release rates listed in Table 3 were calculated using the empirical model described in Section 1.2. This section provides more detail on the model parameters and how to evaluate them.

##### 4.1. Model Parameters

Below is a description of the parameters in Eqs. (1) and (2). The only parameters that vary from enclosure to enclosure are the vent separation height,  $H$ , and the vent inlet, exhaust, and leakage areas,  $A_i$ ,  $A_e$ , and  $A_l$ . The others are either physical or empirical constants.

**Acceleration of gravity:**  $g \approx 9.8 \text{ m/s}^2$

**Ambient density:**  $\rho_0 \approx 1.2 \text{ kg/m}^3$ . The density of air corresponding to a temperature of approximately  $20 \text{ }^\circ\text{C}$  ( $68 \text{ }^\circ\text{F}$ ).

**Heat of combustion:**  $\Delta H_{\text{air}} \approx 3000 \text{ kJ/kg}$ . The heat of combustion based on oxygen consumption for most fuels is within approximately 5 % of  $13100 \text{ kJ/kg}$  [10]. Multiplying this value by the oxygen mass fraction in air, 0.23, yields approximately  $3000 \text{ kJ/kg}$ .

**Discharge coefficient:**  $C \approx 0.61$ , for air flowing through a sharp-edged orifice [11]. Various sources cite values between 0.60 and 0.62 for this parameter, depending on the exact flow conditions. For steel enclosures, the assumption of a sharp-edged orifice is appropriate.

**Non-dimensionalized temperature:**  $\tau \equiv T/T_0 \approx 3$ . This parameter represents the absolute temperature,  $T$ , of the enclosure interior relative to the exterior ambient,  $T_0$ . Based on the measured gas temperatures from the experiments reported here, the actual interior temperature is not uniform and  $\tau$  varies between 2 and 4. However, the air mass flow rate given in Eq. (1) is relatively insensitive to its value, varying only by at most 5 % over this range of temperature.

**Efficiency factor:**  $\chi \approx 0.6$ . This parameter represents the fraction of oxygen drawn into the enclosure that is consumed by the fire. Its chosen value best matches the experimental data, and corresponds to an oxygen concentration in the exhaust stream of approximately 8 %. Mangs and Keski-Rahkonen estimated the value of  $\chi$  to be 0.53 based on their experiments [4]. As shown in the gas species plots in Section C, the oxygen concentration near the top of the enclosure when the peak HRR is reached varies between zero and 10 %, due largely to the specific configuration of the fuel source and enclosure volume and interior make-up. It would be possible to select a more appropriate value for  $\chi$  based on the minimum oxygen concentration achieved in each individual experiment, but this would defeat the point of developing a method for estimating the peak HRR *a priori*.

**Vent separation height:**  $H$  (m). This is the vertical distance between the inlet and exhaust vents. If the enclosure has no vents and only leakage,  $H$  can be taken as 0.63 of the full enclosure height, based on the assumption that the leakage is uniformly distributed and that the magnitude of the air velocity through the gaps increases as the square root of the vertical distance from the neutral plane height; that is, the height at which the air flow changes direction.

**Inlet and exhaust vent areas:**  $A_i, A_e$  ( $\text{m}^2$ ). Some vents, like those shown in Fig. 11, can be measured directly, and some, like those shown in Fig. 12, can be estimated by measuring the length of each louver and multiplying by the opening width. The louvers for Enclosure #3 are approximately 2.6 mm (0.10 in) wide and those for Enclosure #4 are approximately 5.6 mm (0.22 in) wide. These estimates were obtained from the pressure testing results. In lieu of that, the louver width can be estimated using something like a calibrated rod.

**Leakage area:**  $A_l$  ( $\text{m}^2$ ). For the experiments described in this report, the leakage area was obtained using a calibrated fan and pressure transducer. If it is not possible to do this, the leakage area can be estimated by measuring the total length of all of the enclosure's seams, door cracks, etc., and then multiplying this result by 1 mm (0.04 in) after converting to consistent units of length. The effective width of the seams and door cracks, 1 mm, is an average of the measurements of Enclosures #3

through #8 listed in Table 2. Enclosures #1 and #2 had large doors in front and back that had been damaged over time and the door gaps were clearly larger than they would have been when installed.

Consider the enclosure pictured in Fig. 9. This enclosure sits outside of the laboratory where the experiments were conducted, and it was not part of the study. It is merely an example. If one were to estimate the leakage area of this enclosure, one would measure the length of the door perimeter, the perimeter of the foundation, and all other seams where two sheets of steel overlap or abut. Leakage includes knock-outs, bolt holes, gaps, and other openings like those shown in the right photograph of Fig. 10. The vents in this example are the louvers in the side wall whose area can be estimated by measuring the length and width of the openings shown in the left photograph of Fig. 10.

This example points out an important consideration in applying this simple model. Notice that the enclosure is connected by a duct to other enclosures to the left. Unless one has specific information as to the opening area of the duct, the vent and leakage areas of all connected enclosures should be assumed to potentially supply a fire with oxygen. After assessing these additional areas, the calculated fire size may be so large that the assumption of a “closed” enclosure is inappropriate.



**Fig. 9.** Photograph of large outdoor electrical enclosure.



**Fig. 10.** Louvers and miscellaneous leakage paths (yellow lines).

## 4.2. Applying the Model

This section details how one estimates the maximum heat release rate of a fire within a closed steel enclosure using the Mangs and Keski-Rahkonen model described above. This procedure was used to estimate the values under the title “Max HRR, model” listed in Table 3.

1. Measure the areas of the inlet and exhaust vents,  $A_i$  and  $A_e$ . If there is uncertainty as to whether a particular vent is an inlet or exhaust, assume the neutral plane to be halfway up the height of the enclosure and that vents lower than this are inlet and vents higher are exhaust. An exception to this rule would be where there is a hole in the ceiling and a single vent in the wall near the top of the enclosure. In this case, the hole in the ceiling is the exhaust vent and the vent in the wall is the inlet vent.
2. Estimate the leakage area,  $A_l$ . Unless there is some obvious concentration of leakage near the top or bottom of the enclosure, add half of the leakage area to the inlet area,  $A_i$ , and half to the exhaust area,  $A_e$ .
3. Measure the height,  $H$ , between the centers of the lower and upper vents.
4. Compute the mass flow rate of air through the vent,  $\dot{m}$ , from Eq. (1), assuming that  $C = 0.61$ ,  $\rho_0 = 1.2 \text{ kg/m}^3$ ,  $g = 9.8 \text{ m/s}^2$ , and  $\tau = 3$ .
5. Compute the expected maximum heat release rate,  $\dot{Q}_{\max}$  (kW), from Eq. (2), assuming that  $\chi = 0.6$  and  $\Delta h_{\text{air}} = 3000 \text{ kJ/kg}$ .

If the estimated peak HRR exceeds 250 kW, it might be worth examining the construction of the enclosure. In the experiments reported here, fires in excess of 250 kW heated the enclosure panels significantly, causing additional leakage. It was not possible to measure the increased leakage, but it was observed that doors warped, instrument panels melted, and screws popped open as the steel temperatures rose. Some enclosures, like motor control cabinets, have relatively small panels that did not appear to warp, but the larger switchgear cabinets have relatively large doors and panels whose seams appeared to open significantly. If the estimated peak HRR is relatively low, the enclosure openings will most likely not change.

In the first two experiments performed on Enclosure #5, a number of events occurred that were not planned. First, plastic components of several instrument panels melted and fell inside the cabinet, allowing more air to flow in and adding to the combustible load. Second, some large steel panels opened up because they were not screwed securely to the frame. Some screws were simply missing and went unnoticed. This enclosure was relatively well-ventilated and its estimated peak HRR was 289 kW, a relatively large fire for such a confined space that led to temperatures high enough to compromise its structural integrity.

## 5. Conclusion

Experiments have been performed to validate an empirical correlation that estimates the maximum heat release rate of a fire within a closed steel enclosure. The model was developed by Mangs and Keski-Rahkonen of VTT Finland [4]. Using the results of 29 experiments, the model has been shown to under-predict the measured maximum heat release rate by approximately 4 %. The relative standard uncertainty of the model's prediction is 25 %. The uncertainty in model prediction is largely due to the uncertainty in the measured leakage area of the enclosure.

In applying the model in practice, it is important to account for the fact that the leakage and ventilation area of a large enclosure might support a fire with a heat release rate of several hundred kilowatts, and such a fire can induce more leakage that could sustain a larger fire. This might be the case for enclosures with large panel doors or control equipment that could potentially melt and drop out.

It is also important to note that a nominally small amount of ventilation and leakage can support a fire that generates a significant amount of heat and unburned fuel vapors which can lead to a substantially larger fire if a door or panel is suddenly opened; for example, by first responders. This was demonstrated in one of the experiments, where a door was intentionally opened after an *ad hoc* sprinkler system failed to suppress a fire.

## 6. References

- [1] R.P. Kassawara and J.S. Hyslop. EPRI/NRC-RES Fire PRA Methodology for Nuclear Power Facilities: Detailed Methodology. NUREG/CR-6850, United States Nuclear Regulatory Commission, Washington, DC, 2005.
- [2] IEEE, New York, NY. *IEEE 383, IEEE Standard for Qualifying Electric Cables and Splices for Nuclear Facilities*, 2015.
- [3] J.M. Chavez and S.P. Nowlen. An Experimental Investigation of Internally Ignited Fires in Nuclear Power Plant Control Cabinets, Part II: Room Effects Tests. NUREG/CR-4527 (SAND86-0336), Sandia National Laboratory, Albuquerque, New Mexico, November 1988. Work performed under contract to the US Nuclear Regulatory Agency, Washington DC.
- [4] J. Mangs and O. Keski-Rahkonen. Full-scale fire experiments on electronic cabinets. VTT Publications 186, VTT Technical Research Centre of Finland, Espoo, Finland, 1994.
- [5] J. Mangs and O. Keski-Rahkonen. Full-scale fire experiments on electronic cabinets II. VTT Publications 269, VTT Technical Research Centre of Finland, Espoo, Finland, 1996.
- [6] J. Mangs. On the fire dynamics of vehicles and electrical equipment. VTT Publications 521, VTT Technical Research Centre of Finland, Espoo, Finland, 2004.
- [7] K. McGrattan and S. Bareham. Heat Release Rates of Electrical Enclosure Fires (HELEN-FIRE). NUREG/CR-7197, United States Nuclear Regulatory Commission, Washington, DC, 2015.
- [8] A. Lindeman and M.H. Salley. Refining And Characterizing Heat Release Rates From Electrical Enclosures During Fire (RACHELLE-FIRE), Volume 1: Peak Heat Release Rates and Effect of Obstructed Plume. NUREG-2178, United States Nuclear Regulatory Commission, Washington, DC, April 2016.
- [9] G. Taylor, A.D. Putorti, and C. LaFleur. Report on High Energy Arcing Fault Experiments, Experimental Results from Medium Voltage Electrical Enclosures. NRC Research Information Letter (RIL) 2021-10, U.S. Nuclear Regulatory Commission (NRC), Washington, D.C., 2021.
- [10] M. Janssens. *SFPE Handbook of Fire Protection Engineering*, chapter Calorimetry. National Fire Protection Association, Quincy, Massachusetts, 5th edition, 2015.
- [11] M.S. Owen. *2009 ASHRAE Handbook: Fundamentals*. American Society of Heating, Refrigerating, and Air-Conditioning Engineers, Inc., Atlanta, GA, 2009.

## A. Model Derivation

This section provides the derivation of Eq. (1).

Consider an enclosure with ventilation openings near the bottom (inlet) and top (exhaust), separated by a vertical distance,  $H$ . The pressure just outside of the inlet vent is taken as  $p_0$ ; the pressure drop across the inlet vent,  $\Delta p_i$ ; the pressure drop across the exhaust vent,  $\Delta p_e$ ; the gas density outside the enclosure  $\rho_0$ ; and the gas density inside  $\rho$ . The following equation relates these quantities by asserting that the pressure just outside of the exhaust vent can be calculated by following a path either inside or outside of the enclosure:

$$p_0 - \Delta p_i - \rho gH - \Delta p_e = p_0 - \rho_0 gH \quad (4)$$

It is assumed that the mass of gases flowing into the inlet vent and out of the exhaust vent is the same:

$$\dot{m} \equiv C_i A_i \sqrt{2\rho_0 |\Delta p_i|} = C_e A_e \sqrt{2\rho |\Delta p_e|} \quad (5)$$

where  $C_i$  and  $C_e$  are the orifice coefficients and  $A_i$  and  $A_e$  are the areas of the inlet and exhaust vents, respectively. The equation of state for an ideal gas is given by:

$$p = \mathcal{R} \rho T / W \quad (6)$$

where  $\mathcal{R}$  is the universal gas constant and  $W$  is the molecular weight of the gas. Because the total pressure,  $p$ , inside and outside the enclosure varies by a very small amount, and assuming that the molecular weight of the gases varies by a small amount, it is assumed that

$$\frac{\rho_0}{\rho} \approx \frac{T}{T_0} \equiv \tau \quad (7)$$

where  $T$  is the (absolute) temperature inside the enclosure and  $T_0$  outside. Defining

$$\mu = \left( \frac{C_i A_i}{C_e A_e} \right)^2 \quad (8)$$

and using Eq. (4) to substitute out  $\Delta p_i$ , Eq. (5) can be rewritten as

$$|\Delta p_e| = \mu \tau |\Delta p_i| = \frac{\mu(\tau - 1)\rho_0 gH}{1 + \mu\tau} \quad (9)$$

Assuming that the discharge coefficients are equal ( $C = C_i = C_e$ ), Eq. (5) now becomes:

$$\dot{m} = C \rho_0 \sqrt{2gH} \sqrt{\frac{1 - 1/\tau}{1/A_i^2 + \tau/A_e^2}} \quad (10)$$

## B. Enclosure Drawings

Enclosures #1 and #2 (rear, 1.52 m [60 in] deep)

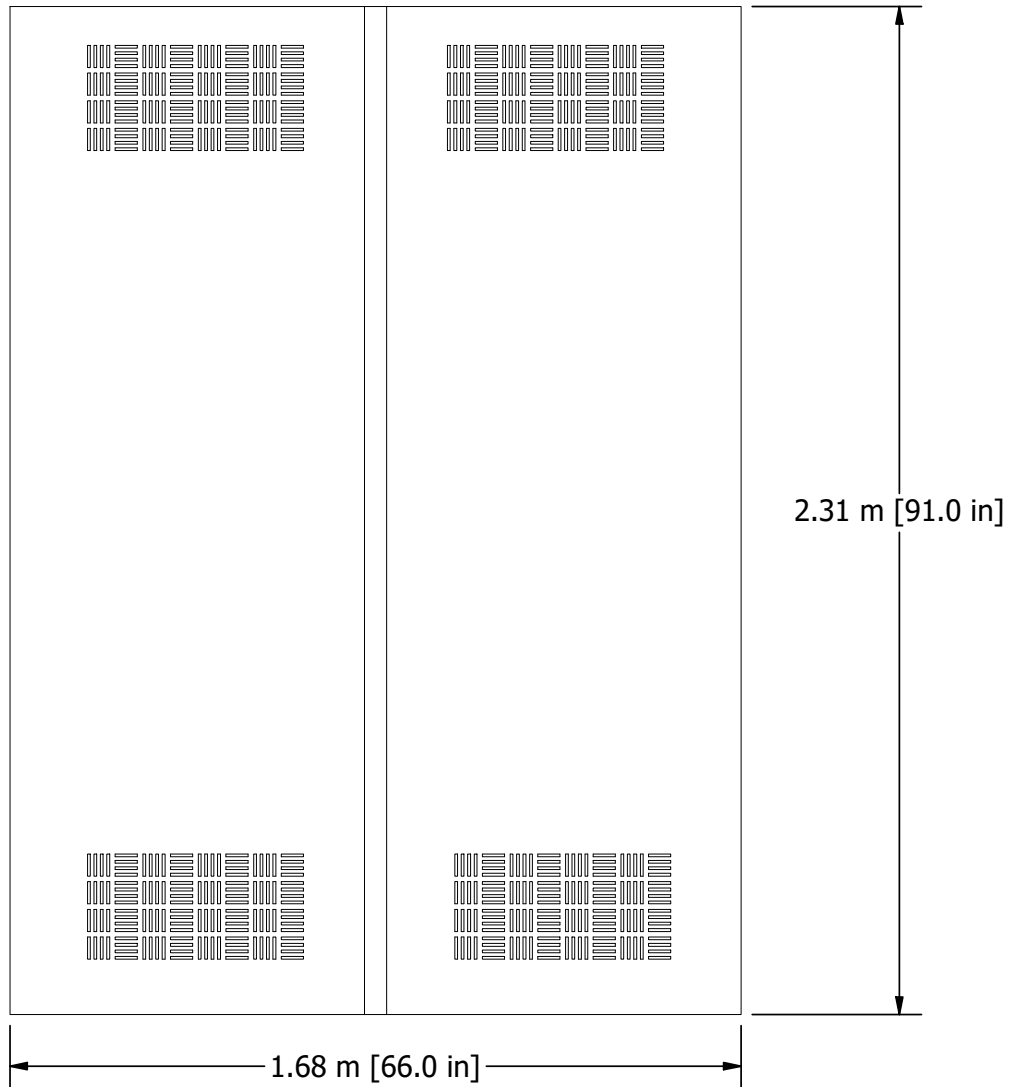


**Fig. 11.** Sketch of Enclosure #1 and #2.

Enclosure #3 (1.40 m [55 in] deep)

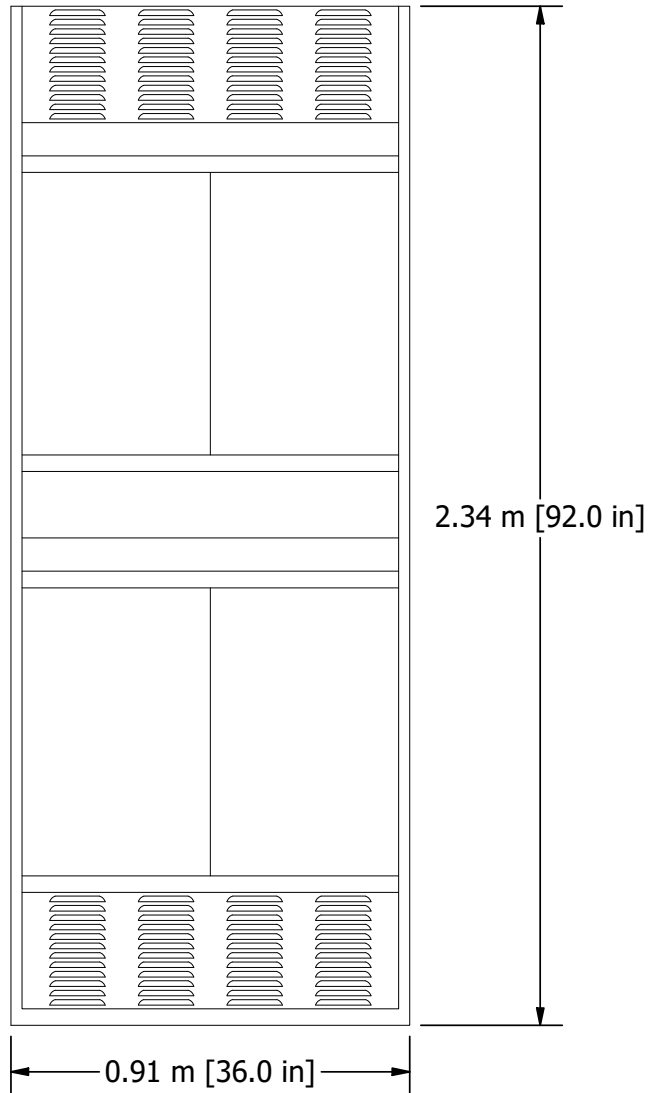
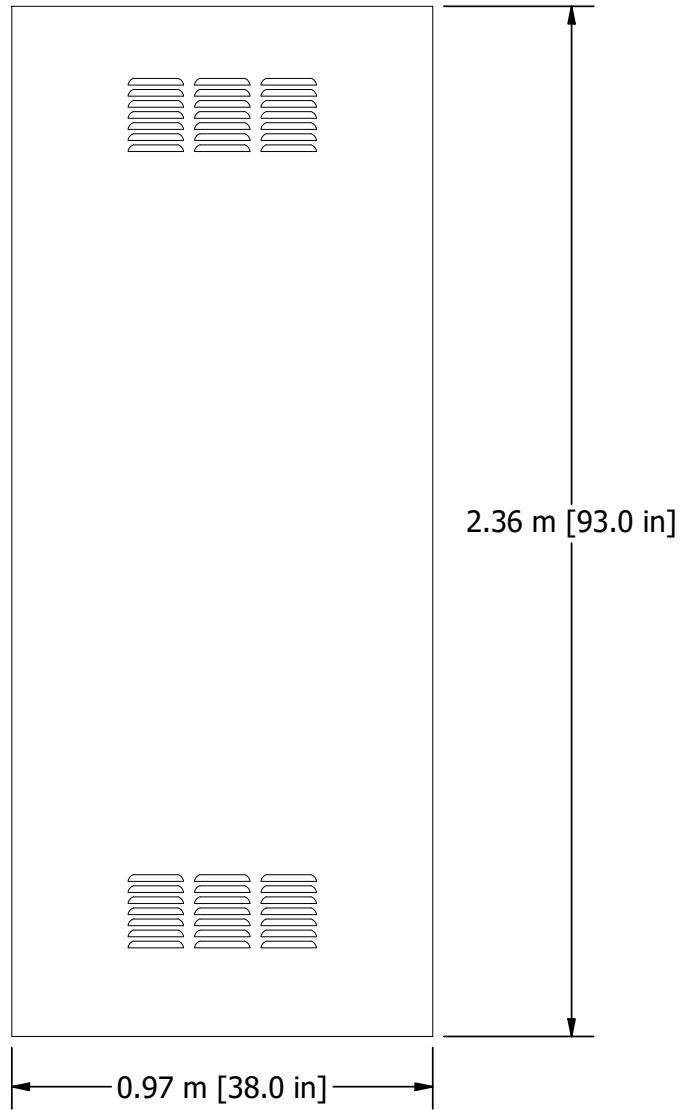


Fig. 12. Sketch of Enclosure #3.

Enclosure #4 (rear) (1.56 m [62 in] deep)



**Fig. 13.** Sketch of Enclosure #4.

Enclosure #5 (1.37 m [54 in] deep)

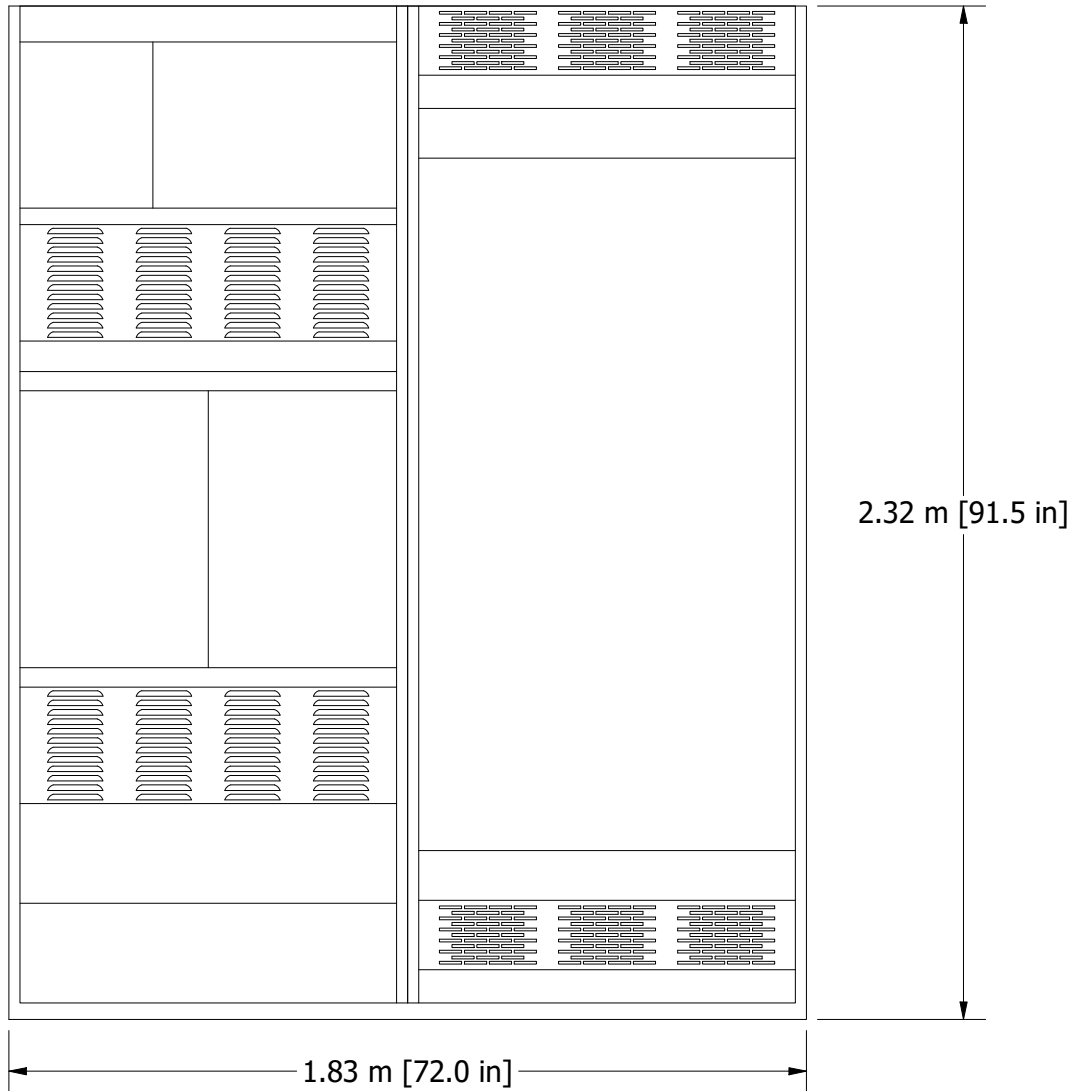
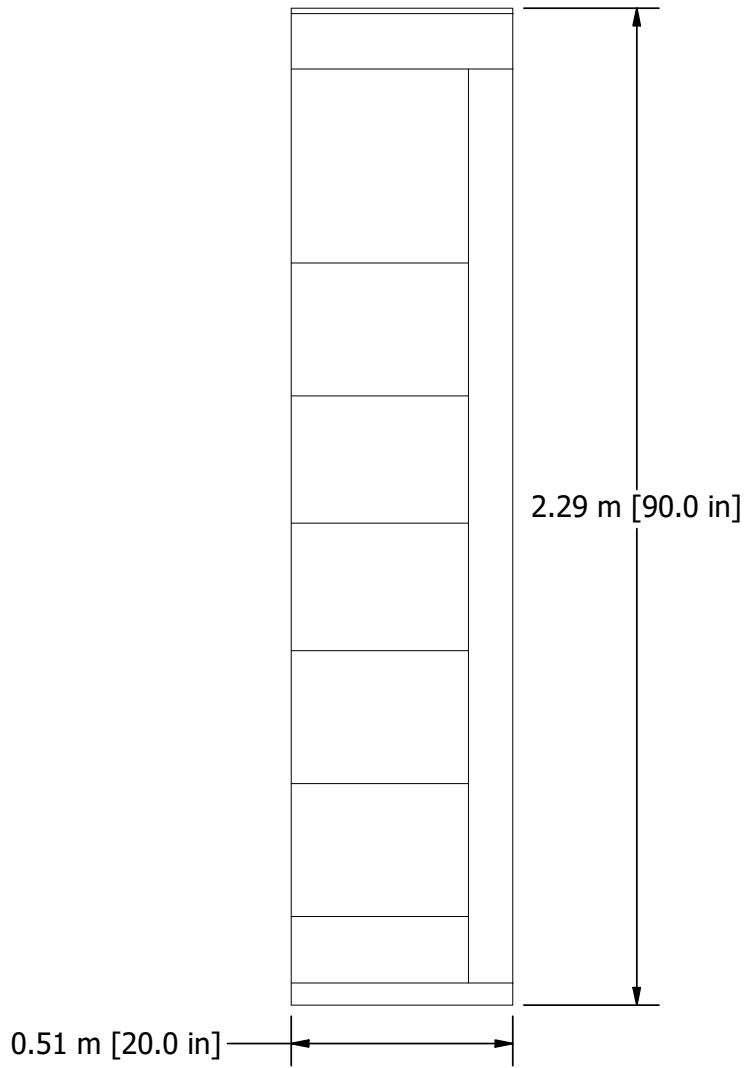
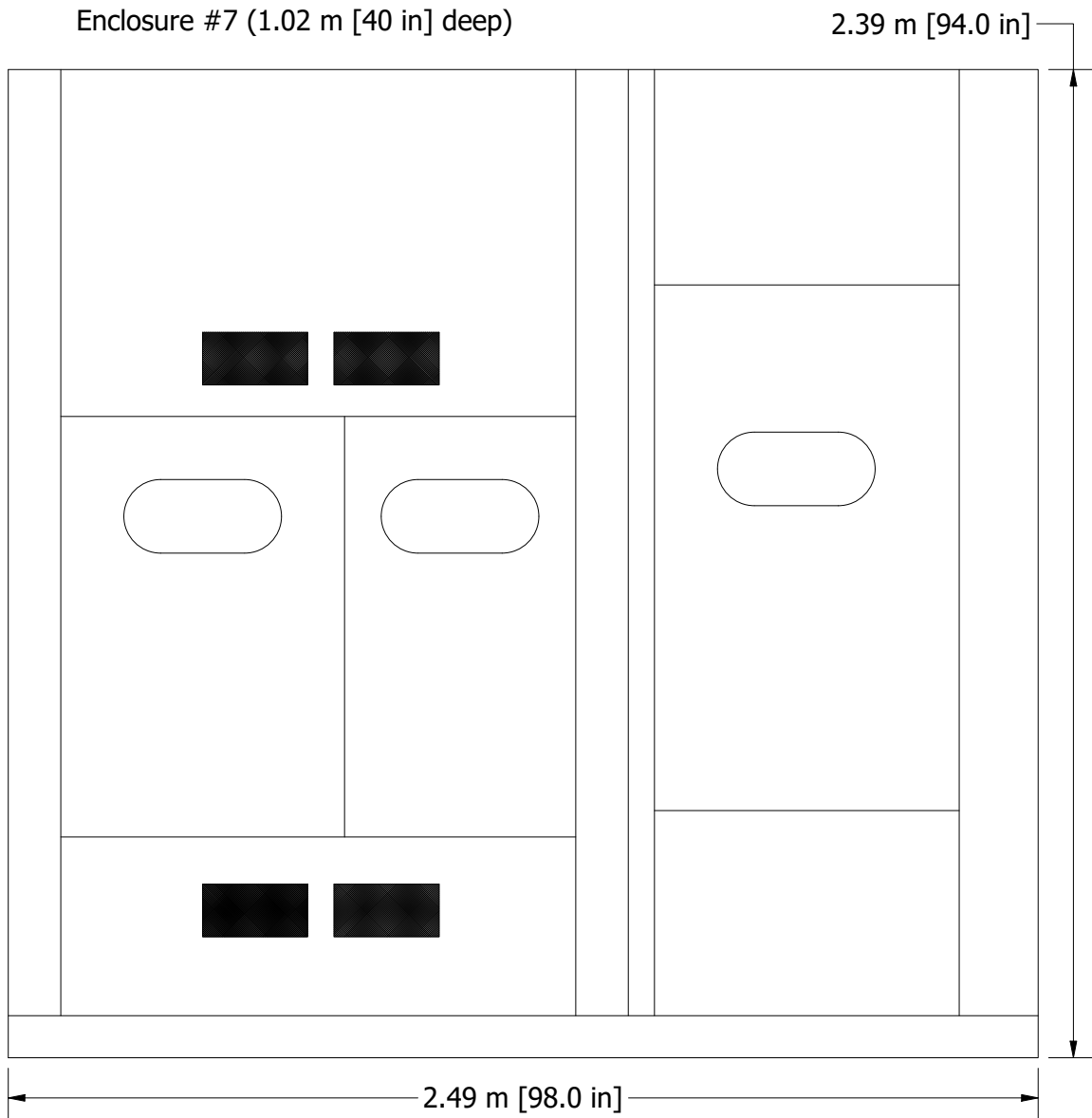


Fig. 14. Sketch of Enclosure #5.

Enclosure #6 (0.36 m [14 in] deep)



**Fig. 15.** Sketch of Enclosure #6.



**Fig. 16.** Sketch of Enclosure #7.

Enclosure #8 (0.51 m [20 in] deep)

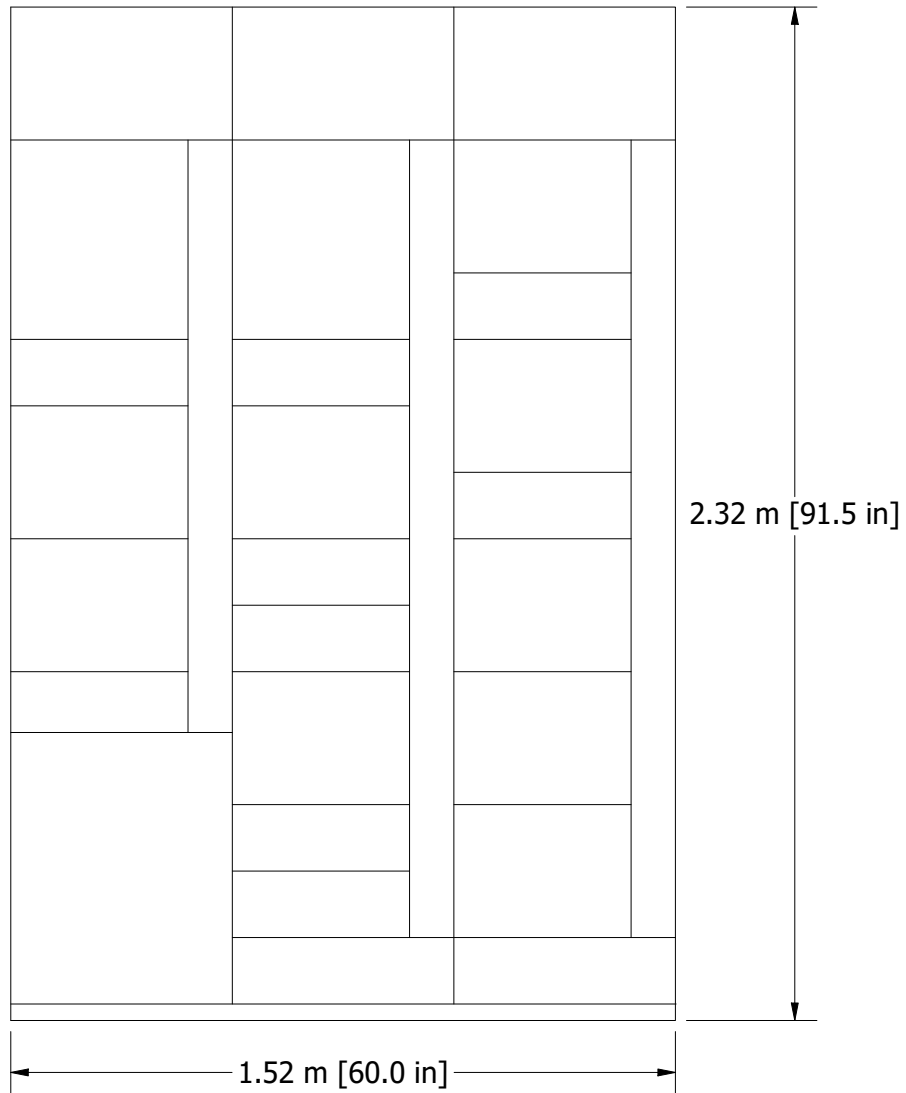


**Fig. 17.** Sketch of Enclosure #8.

### **C. Summary of Experiments**

This section contains a brief description of each experiment. The heat release rate (HRR) plot for the experiments involving a natural gas burner consists of two curves. The dashed line, labelled “Ideal,” is the HRR that would have been achieved had all of the metered natural gas been consumed. The solid line, labelled “Actual,” is the HRR that was actually measured using oxygen consumption calorimetry. In experiments with solid fuels, the dashed curve represents the theoretical HRR of the metered natural gas igniter and the solid curve represents the HRR of both the igniter and solid fuel as measured using oxygen consumption calorimetry.

The measurements of oxygen, carbon dioxide, and carbon monoxide were made by extracting a gas sample from a point approximately 30 cm below the ceiling of the enclosure.

### C.1. Experiment 1

The 30 cm by 30 cm natural gas burner was positioned in the right, front section of Enclosure #5, as shown in Fig. 18. The heat release rate was stepped up in increments of approximately 50 kW. Even though the near-ceiling oxygen concentration approached zero, the fuel gases burned inside and outside of the enclosure, and the fire's measured HRR did not deviate from its theoretical value. Notice that the steel panel on the upper right side of the enclosure opened unexpectedly, and the fire burned outside of the upper vent and opened side panel. For this reason, this experiment was not used to validate the empirical model because of the unexpected breach.

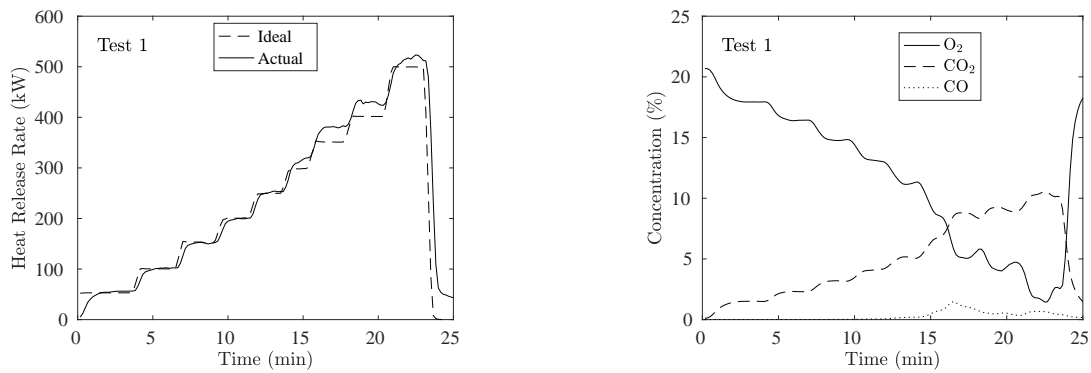
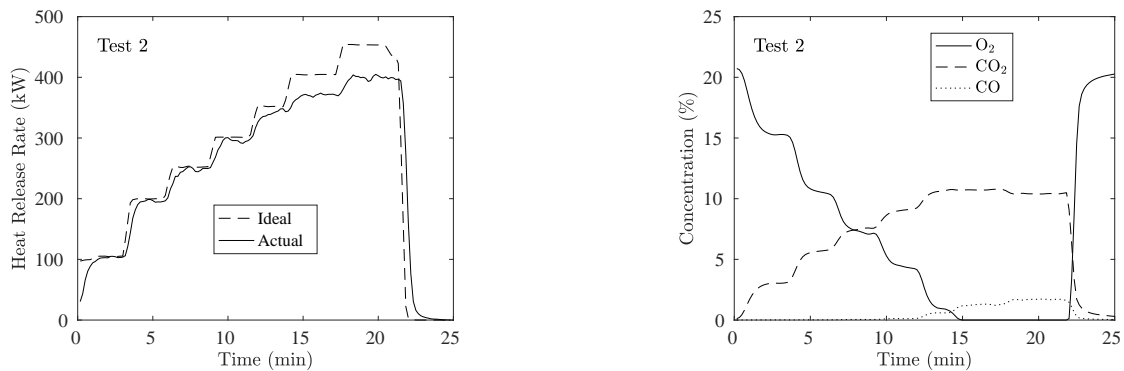


Fig. 18. Heat release rate, gas concentrations, and photograph of Experiment 1.

## C.2. Experiment 2

Experiment 2 was a repeat of Experiment 1. The opened panel on the right side was secured, but some noticeable opening still occurred. The HRR reached approximately 400 kW and the oxygen concentration dropped to zero. This experiment was not used to validate the empirical model because of the unexpected breach and uncertainty in the actual leakage area during the fire.



**Fig. 19.** Heat release rate, gas concentrations, and photograph of Experiment 2.

### C.3. Experiment 3

The vents on the right section of Enclosure #5 were closed using mineral wool and steel plates as shown in Fig. 20. The burner remained in the front of the right half of the enclosure. The HRR reached approximately 160 kW and the oxygen concentration dropped to nearly zero. No flames emerged from the enclosure.

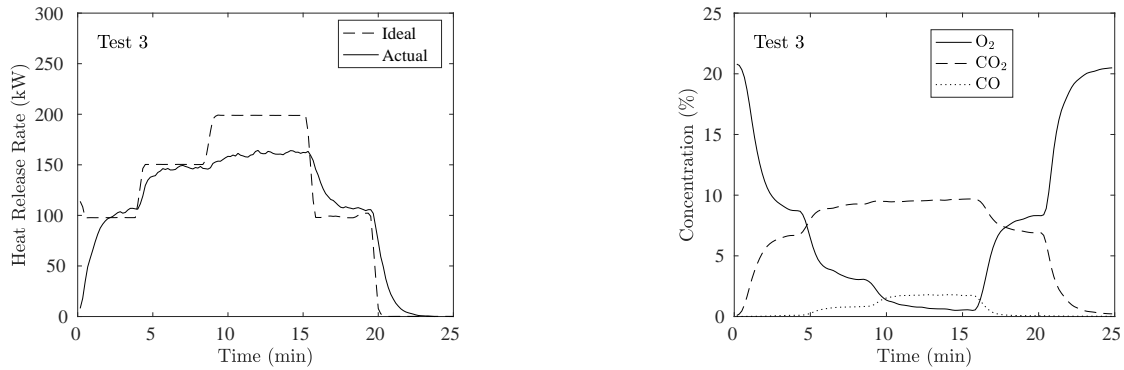


Fig. 20. Heat release rate, gas concentrations, and photograph of Experiment 3.

### C.4. Experiment 4

All of the vents of Enclosure #5 were closed using mineral wool and steel plates as shown in Fig. 21. The burner remained in the front of the right half of the enclosure. The HRR reached approximately 100 kW and the oxygen concentration dropped to approximately 2 %. No flames emerged from the enclosure.

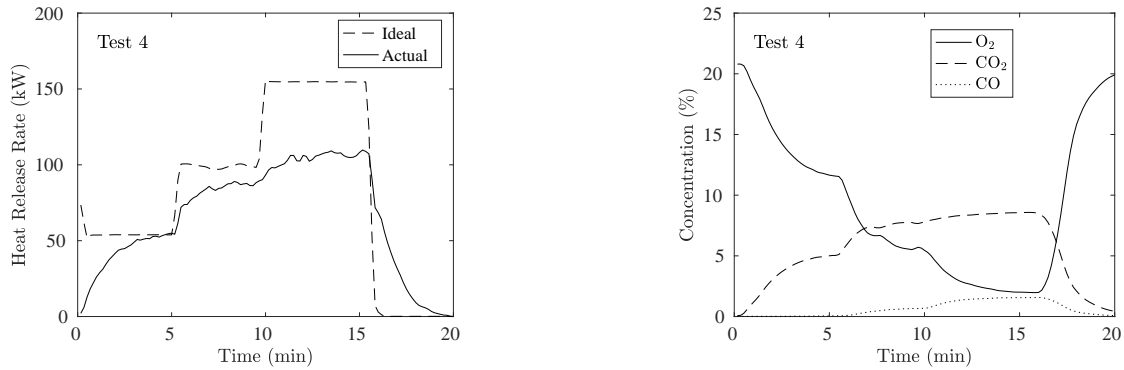


Fig. 21. Heat release rate, gas concentrations, and photograph of Experiment 4.

### C.5. Experiment 5

Experiment 5 was a repeat of Experiment 4, except that the burner was moved to the rear of the left half of Enclosure #5. The gas line entering the enclosure is shown in the photograph of Fig. 22. The results of this experiment were similar to the previous experiment.

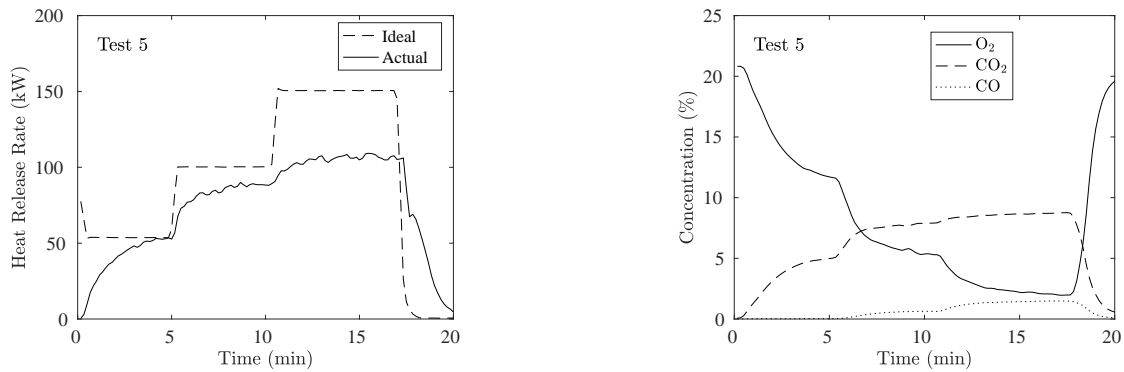
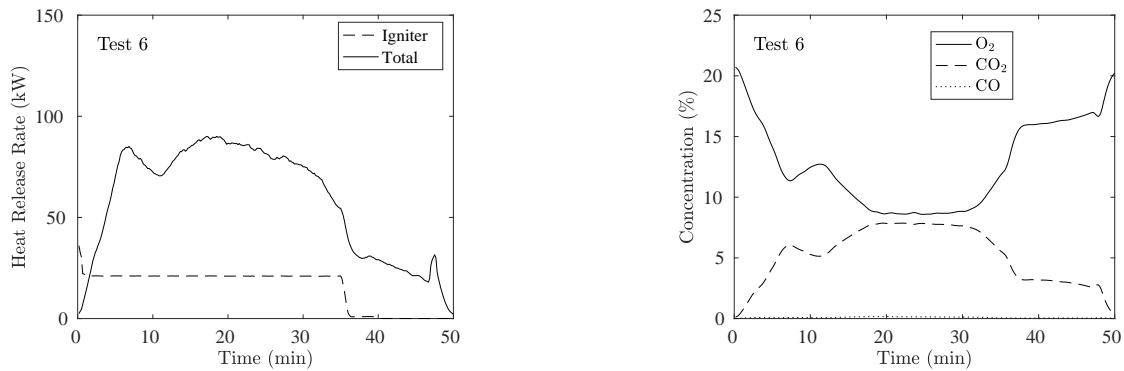


Fig. 22. Heat release rate, gas concentrations, and photograph of Experiment 5.

### C.6. Experiment 6

A 90 cm by 60 cm (3 ft by 2 ft) steel pan filled with several different plastic sheets was placed on bricks on the right side of Enclosure #5. The pile was ignited with a 20 kW natural gas tube burner. A photograph of the burning plastic outside of the enclosure is shown in Fig. 23. Its peak HRR outside was approximately 400 kW, but only reached 80 kW when burned inside the enclosure with its two left vents open and two right vents closed. There was a substantial amount of unburned plastic melt at the end of the experiment.



**Fig. 23.** Heat release rate, gas concentrations, and photograph of Experiment 6. The photograph shows the burning plastic outside of the enclosure.

### C.7. Experiment 7

Experiment 7 was a repeat of Experiment 6, except that all vents were opened and several layers of gypsum board were placed underneath the steel pan to better replicate the configuration of the fire that was conducted outside of the enclosure. In this case, the plastic was nearly all consumed. The photograph in Fig. 24 shows the thick smoke emanating from the upper vent. No flames emerged from the enclosure.

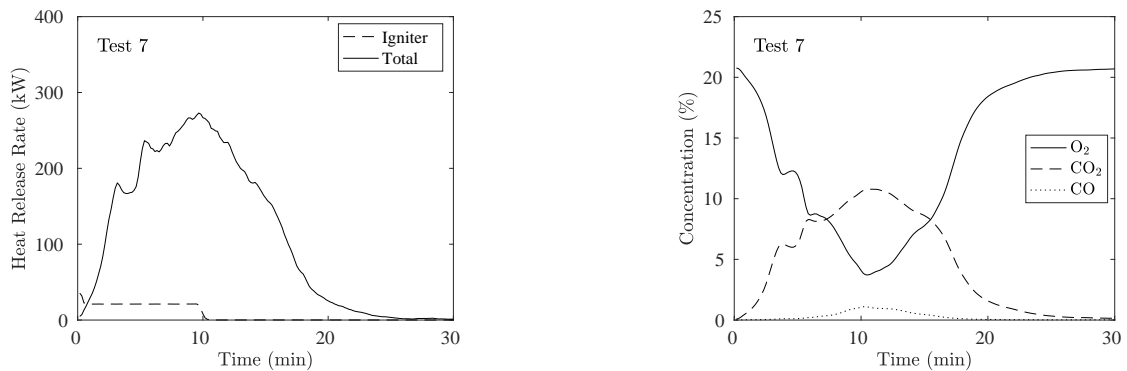


Fig. 24. Heat release rate, gas concentrations, and photograph of Experiment 7.

### C.8. Experiment 8

Experiment 8 was a repeat of Experiments 1 and 2. In both of those previous experiments, the enclosure's panels bulged and opened considerably more than expected because a few critical fasteners had been removed before the enclosure was delivered to the laboratory. The intent of this experiment was to determine if the natural gas fire would reach a maximum HRR comparable to that of the plastics in Experiment 7. Unlike Experiments 1 and 2, there was very limited external flaming because there were no unexpected breaches of the steel panels.

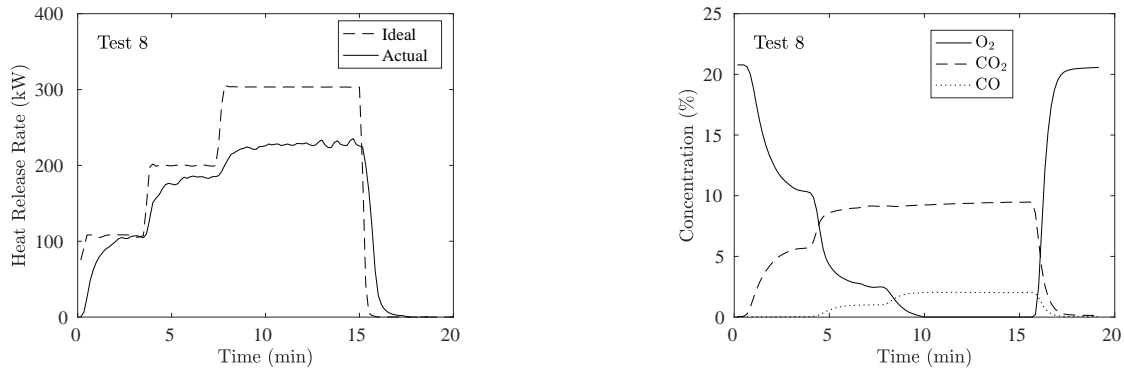
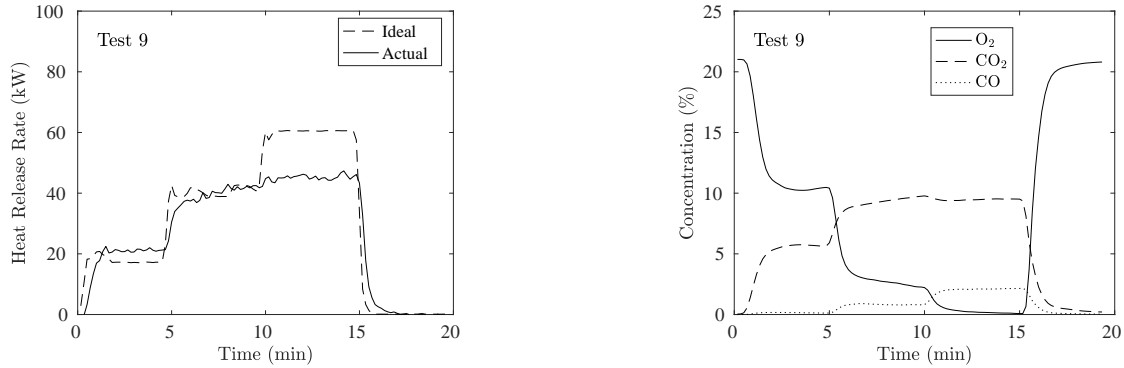


Fig. 25. Heat release rate, gas concentrations, and photograph of Experiment 8.

### C.9. Experiment 9

A photograph of Enclosure #6 is shown in Fig. 26. An 18 cm by 18 cm (7 in by 7 in) natural gas burner was positioned within the lowest compartment of a motor control center (MCC). This enclosure has no vents; only leakage. The gas sampling probe was positioned approximately 8 cm (3 in) from the top. The maximum HRR reached approximately 45 kW.



**Fig. 26.** Heat release rate, gas concentrations, and photograph of Experiment 9. Note the small quartz glass view port cut into the door opening to the lowest compartment where the burner was positioned.

### C.10. Experiment 10

Six electrical cable segments, each approximately 1.8 m (6 ft) long, were hung within the vertical channel on the right side of Enclosure #6 and ignited with a 20 kW tube burner (60 cm long, 2.5 cm diameter steel pipe with holes drilled along its length). The door was left open so that the fully-ventilated fire could be assessed.

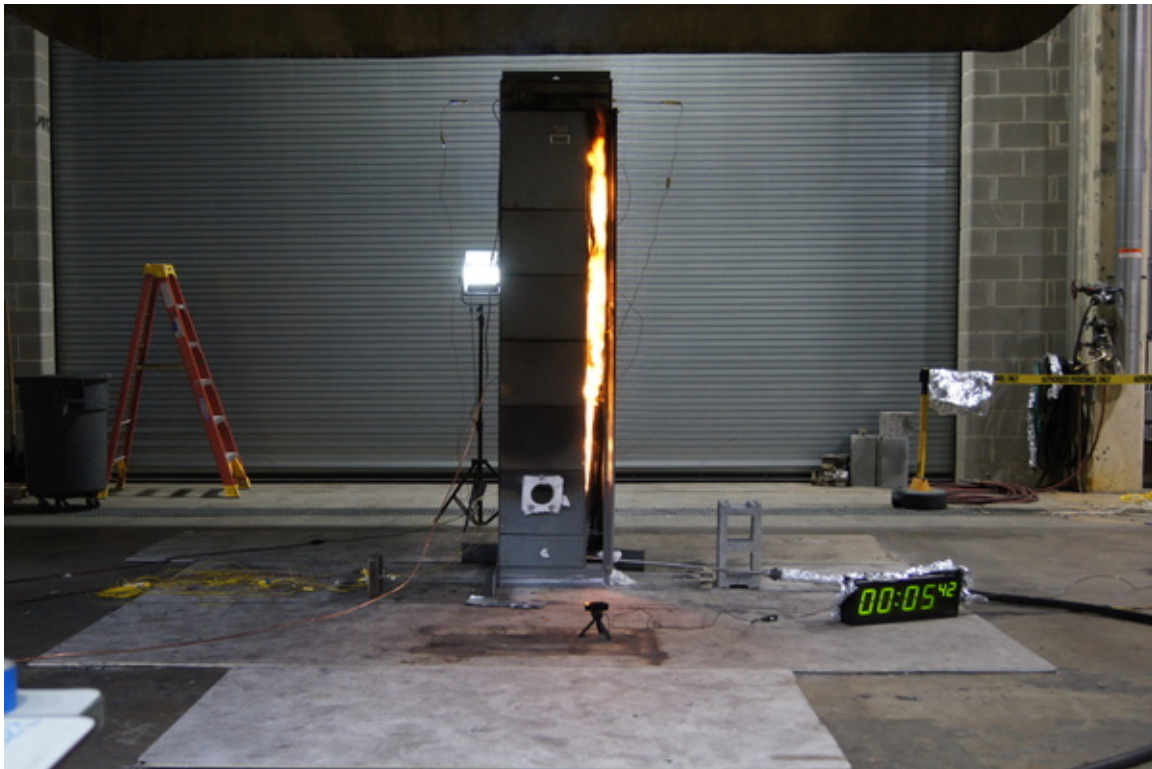
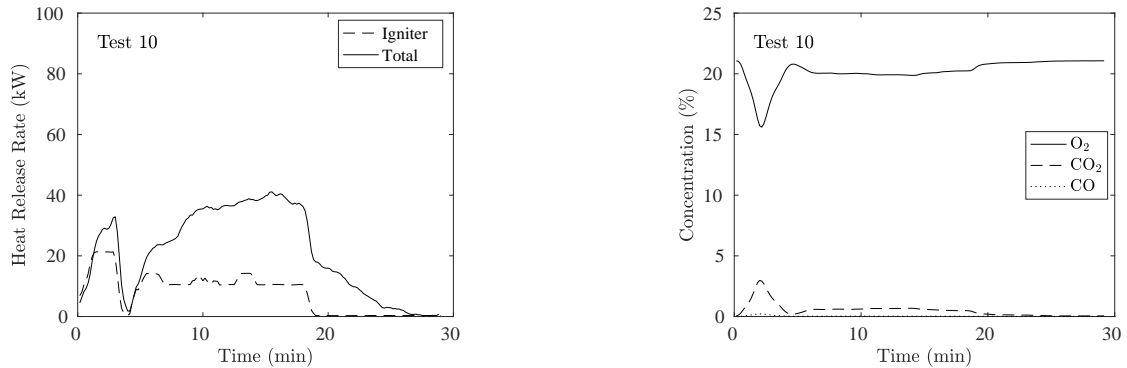
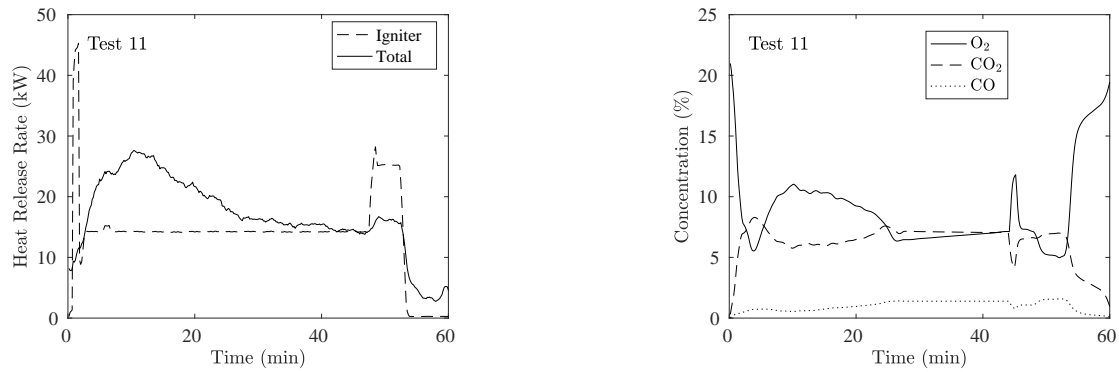


Fig. 27. Heat release rate, gas concentrations, and photograph of Experiment 10.

### C.11. Experiment 11

Experiment 11 was similar to Experiment 10 except that ten cable segments (7 conductor, PE-insulated, PVC-jacketed) were hung within the right vertical channel and the door was closed. Ten cable segments were used rather than six to produce a larger fire that would be certain to reach the ventilation limit of the enclosure.



**Fig. 28.** Heat release rate, gas concentrations, and photograph of Experiment 11. The photograph shows the cables hung along the right channel with a steel pipe burner used to ignite them.

### C.12. Experiment 12

The 30 cm (1 ft) natural gas burner was placed within a large, empty switchgear cabinet, Enclosure #2. With all four vents open, the HRR reached approximately 600 kW.

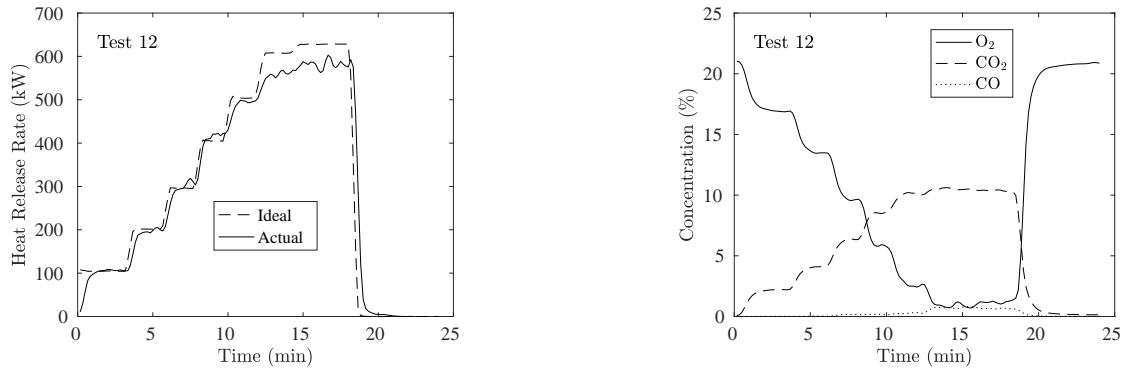
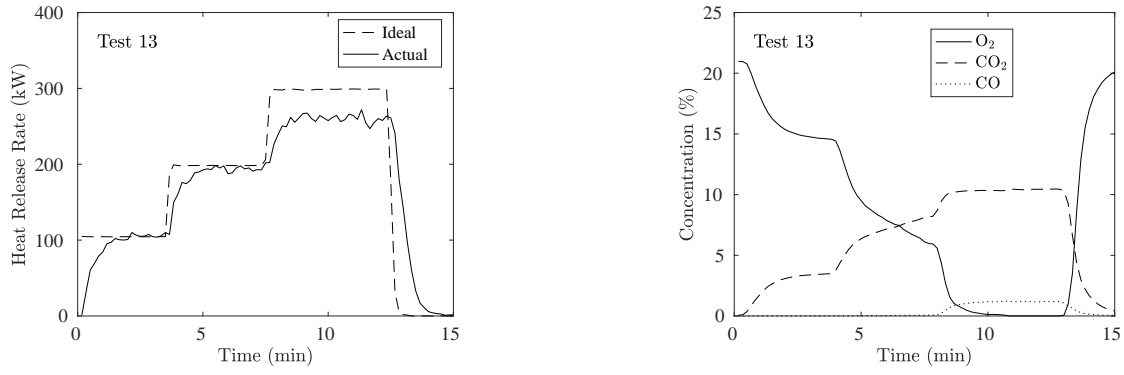


Fig. 29. Heat release rate, gas concentrations, and photograph of Experiment 12.

### C.13. Experiment 13

Experiment 13 was similar to Experiment 12, except that all vents were closed.



**Fig. 30.** Heat release rate, gas concentrations, and photograph of Experiment 13.

### C.14. Experiment 14

A single cardboard box filled with unexpanded polystyrene cups was placed within a steel pan and ignited with three commercially available ethanol-based gel igniters. The photograph in Fig. 31 shows the rear of Enclosure #2 with the box positioned on the right side relative to the front of the enclosure. Outside of the enclosure, this fuel package would reach approximately 600 kW.

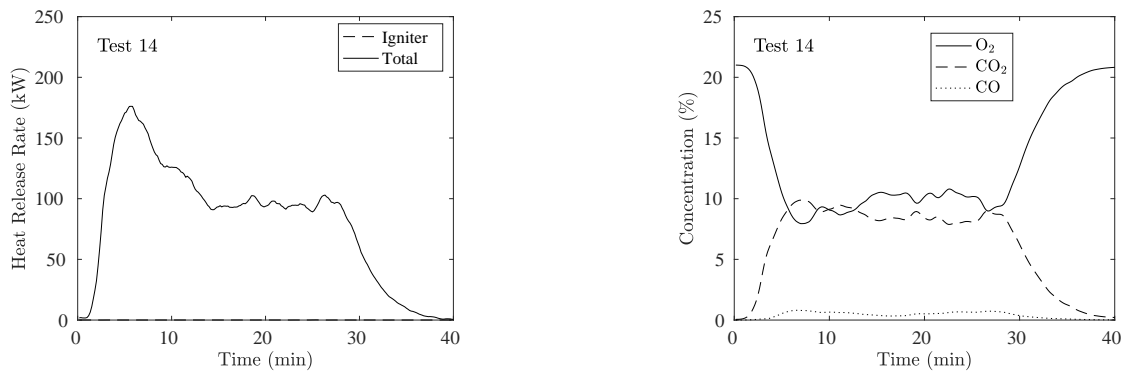


**Fig. 31.** Heat release rate, gas concentrations, and photograph of Experiment 14.

### C.15. Experiment 15

The 30 cm (1 ft) natural gas burner was placed within Enclosure #3 with both of its vents closed. The steel panels that are sealed with red heat-resistant caulk, as shown in the photograph of Fig. 32, cover openings originally used by control panels.

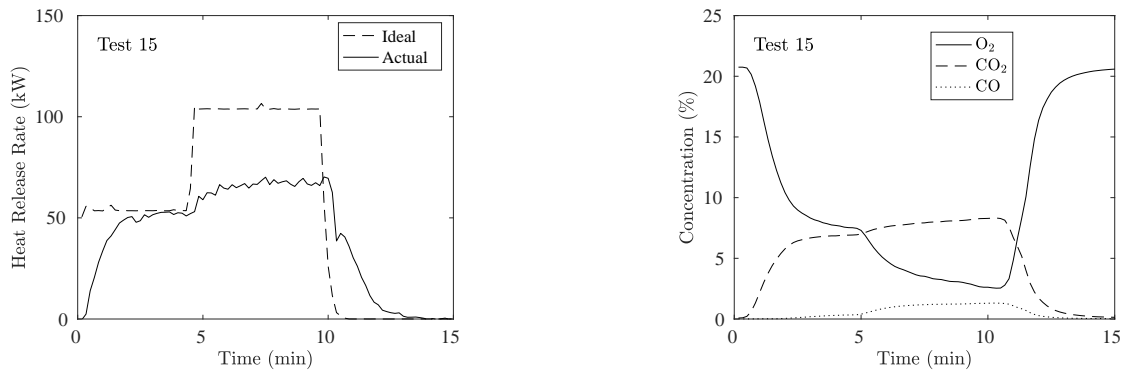


Fig. 32. Heat release rate, gas concentrations, and photograph of Experiment 15.

### C.16. Experiment 16

Experiment 16 was a repeat of Experiment 15 except that the vents were half open, as shown in the photograph of Fig. 33.

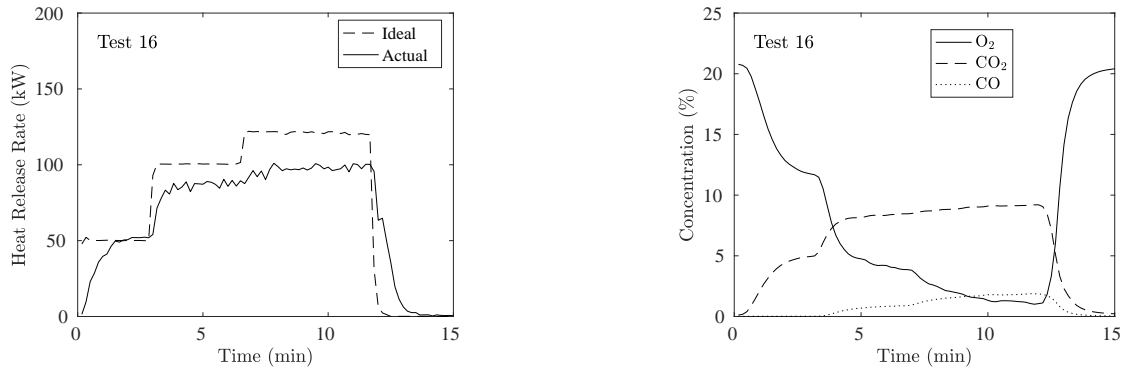


Fig. 33. Heat release rate, gas concentrations, and photograph of Experiment 16.

### C.17. Experiment 17

Experiment 17 was a repeat of Experiment 16 except that the vents were fully open, as shown in the photograph of Fig. 34.

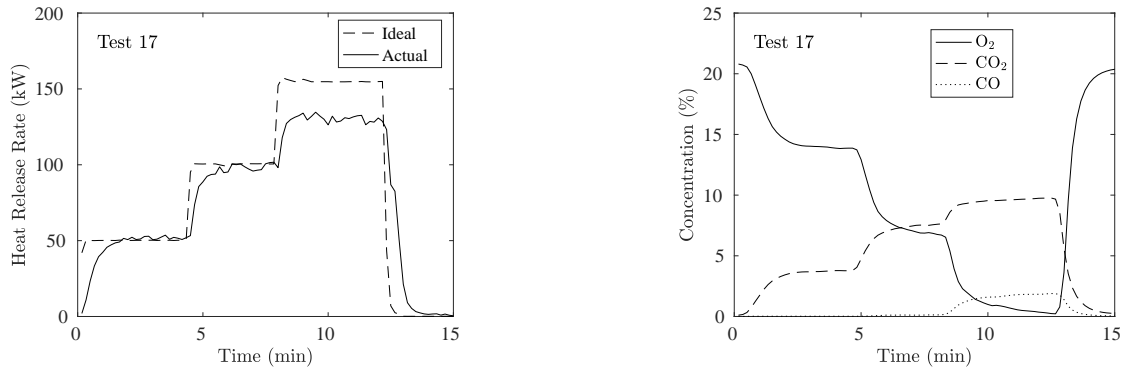


Fig. 34. Heat release rate, gas concentrations, and photograph of Experiment 17.

### C.18. Experiment 18

A tray of assorted plastics was placed within Enclosure #3 with both of its vents open. The plastics, shown in the photograph of Fig. 35, consist of strips of expanded (i.e. foam) and unexpanded (i.e. hard) plastics.

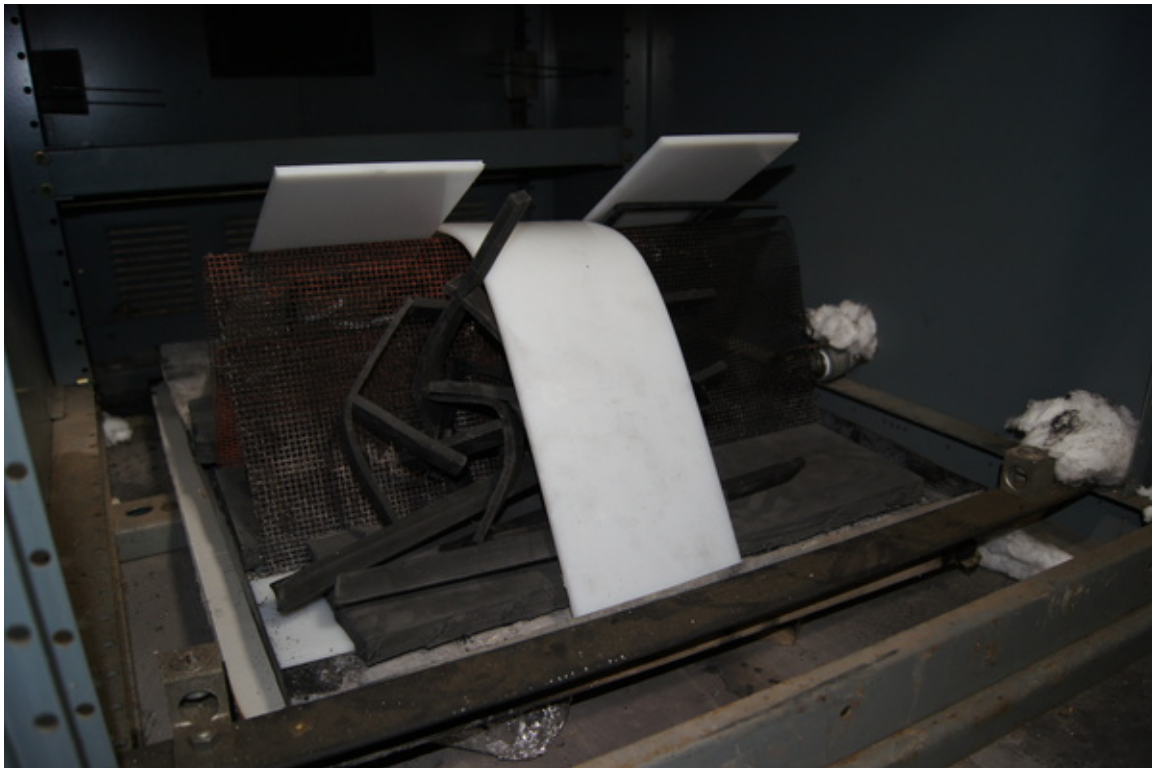
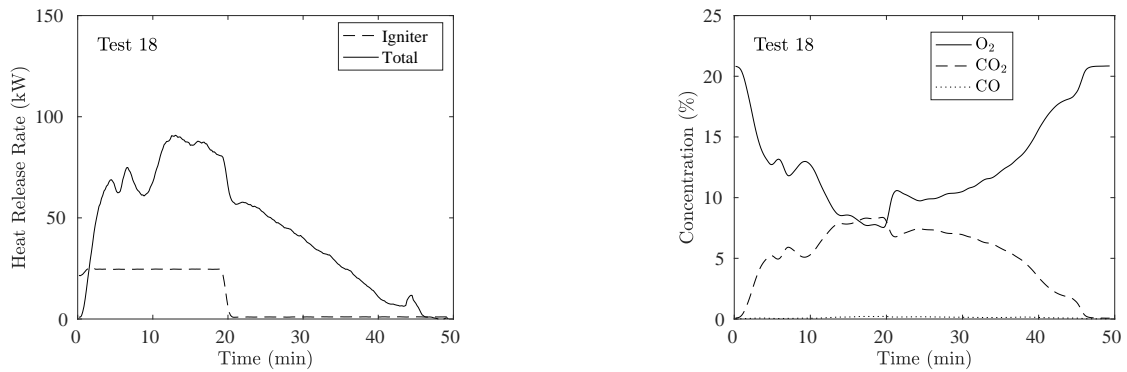


Fig. 35. Heat release rate, gas concentrations, and photograph of Experiment 18.

### C.19. Experiment 19

An 18 cm (7.1 in) square natural gas burner was placed within the lower right compartment of Enclosure #8, a motor control center (MCC) with three vertical columns of compartments that all open up into a common plenum space at the back. The photograph in Fig. 36 shows the position of the burner before the door was closed. The natural gas was piped in from the side.

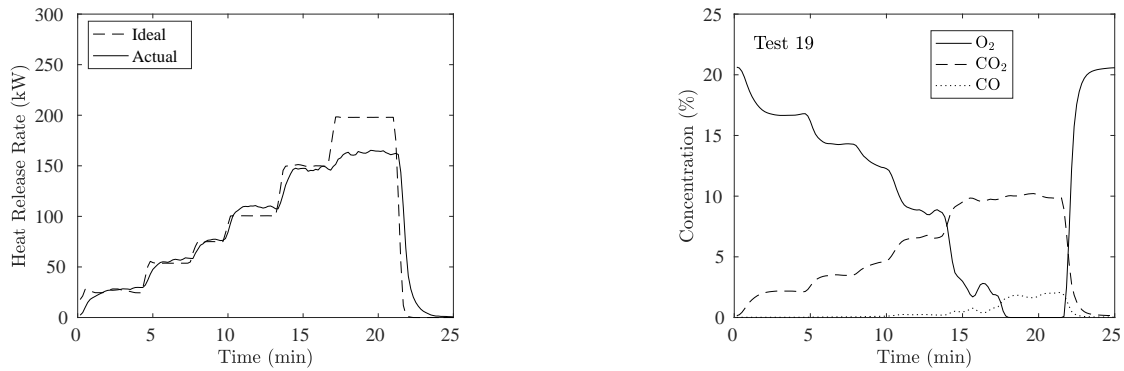
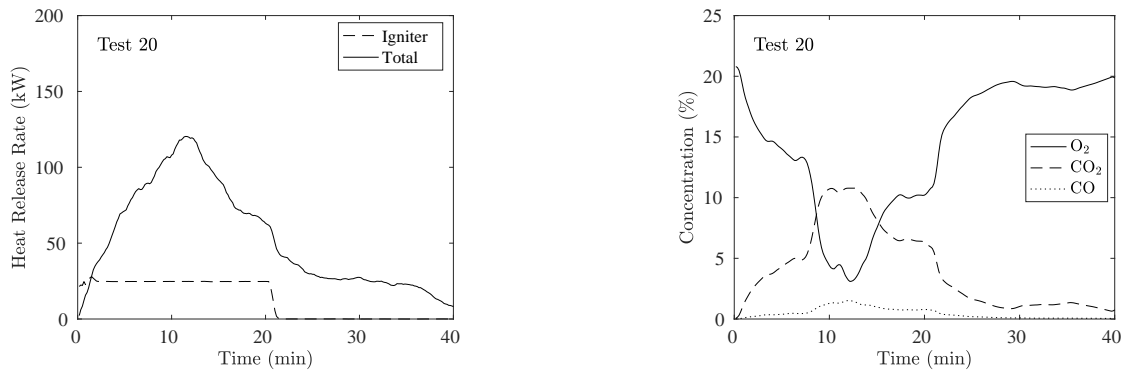


Fig. 36. Heat release rate, gas concentrations, and photograph of Experiment 19.

### C.20. Experiment 20

Twenty-four segments of the same cable used in previous experiments, each 1.8 m (6 ft) long, were hung within the right vertical channel of Enclosure #8. The cables were ignited using a 60 cm (2 ft) long, 2.5 cm (1 in) diameter pipe burner.



**Fig. 37.** Heat release rate, gas concentrations, and photograph of Experiment 20.

### C.21. Experiment 21

Experiment 21 was a repeat of Experiment 20 except that the cables were hung within the center vertical channel of the enclosure. The gap in the gas species measurement at approximately 50 min resulted from a short duration loss in suction.

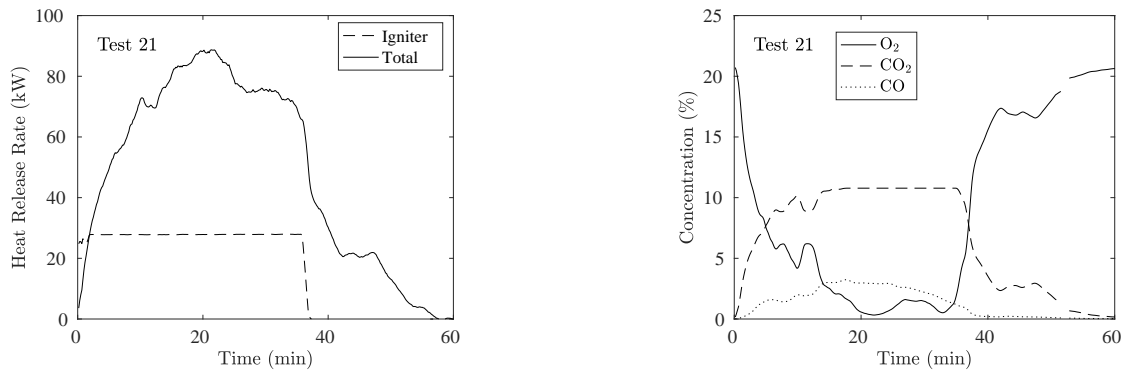


**Fig. 38.** Heat release rate, gas concentrations, and photograph of Experiment 21.

### C.22. Experiment 22

The 30 cm (1 ft) natural gas burner was positioned in the left rear section of Enclosure #7. The vents were open, but steel plates were fastened just inside of the vent openings which blocked most of the air flow.

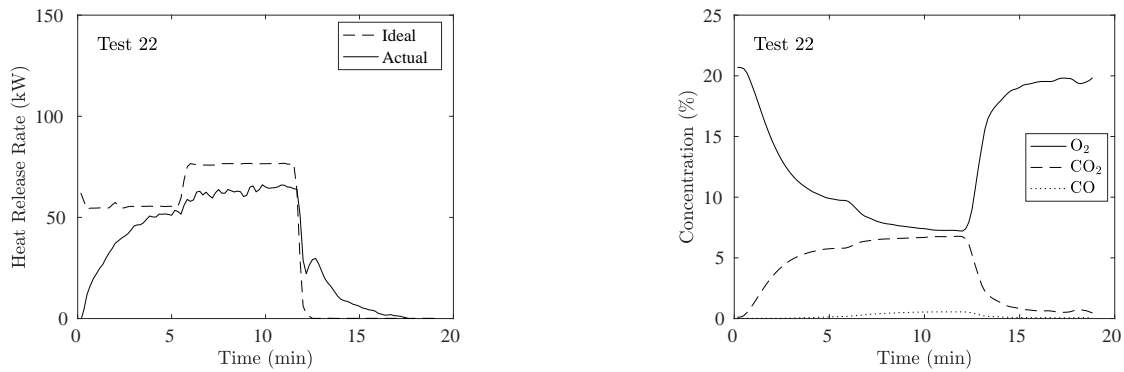
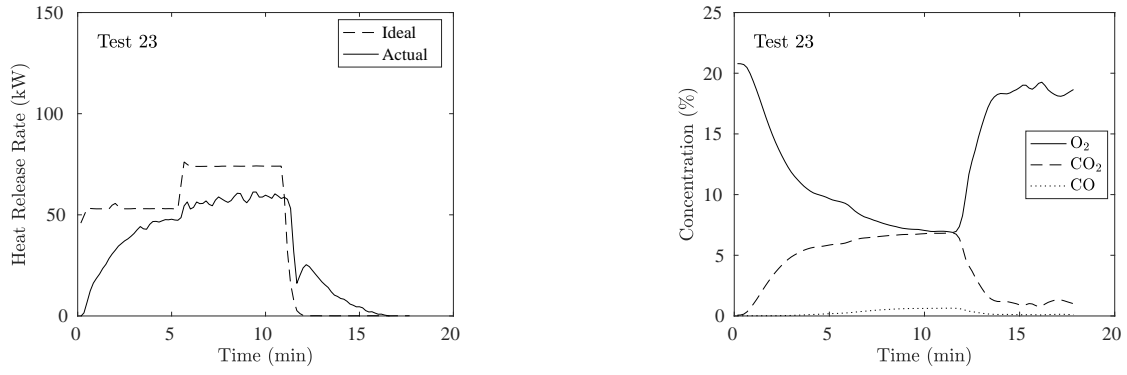


Fig. 39. Heat release rate, gas concentrations, and photograph of Experiment 22.

### C.23. Experiment 23

Experiment 23 was a repeat of Experiment 22, except with two of the four vents covered.



**Fig. 40.** Heat release rate, gas concentrations, and photograph of Experiment 23.

### C.24. Experiment 24

Experiment 24 was a repeat of Experiment 22, except with the steel plates removed from the inside of the vents. The vents were now fully open with no restricted air flow.

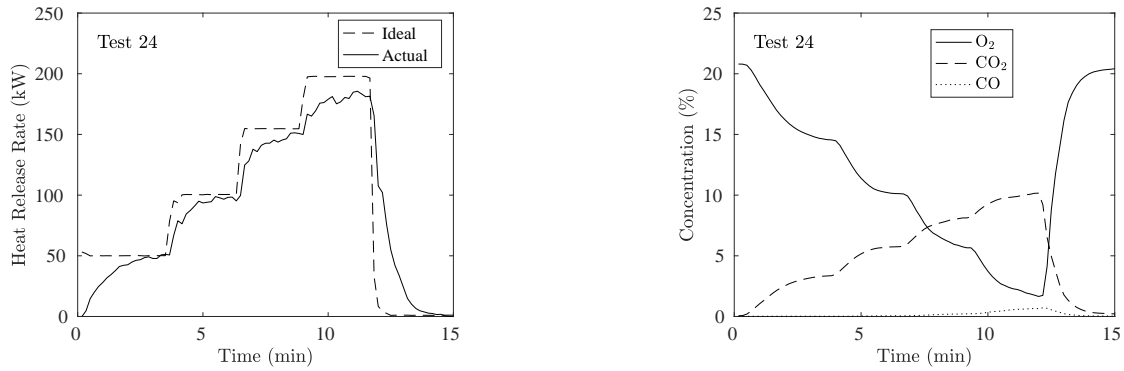


Fig. 41. Heat release rate, gas concentrations, and photograph of Experiment 24.

### C.25. Experiment 25

A tray of approximately 5 kg of assorted plastics was positioned in the left rear section of Enclosure #7. The vents remained fully open.

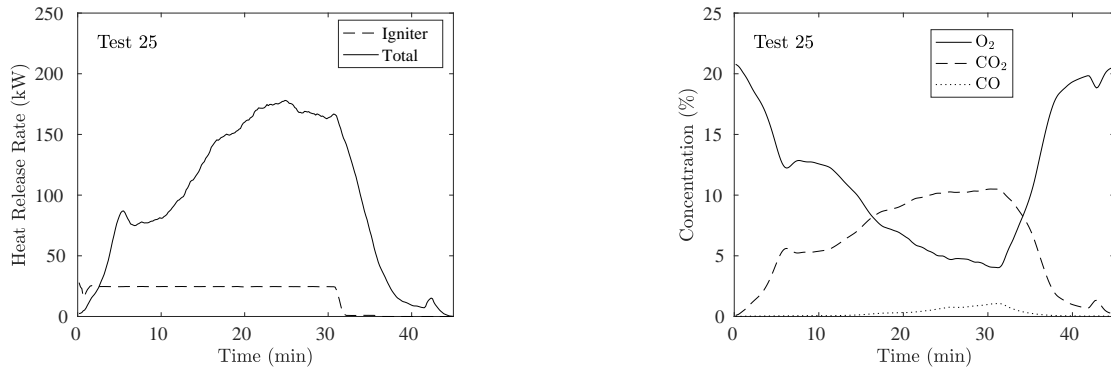


Fig. 42. Heat release rate, gas concentrations, and photograph of Experiment 25.

### C.26. Experiment 26

The 30 cm (1 ft) natural gas burner was positioned in the rear of Enclosure #4 (to the right of the photograph shown in Fig. 43).

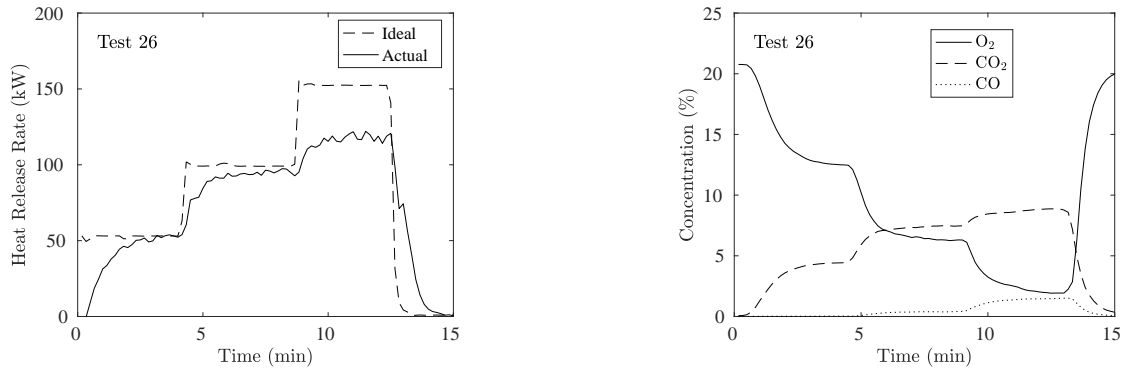


Fig. 43. Heat release rate, gas concentrations, and photograph of Experiment 26.

### C.27. Experiment 27

Experiment 27 was a repeat of Experiment 26, except that the protective dust/insect screen was removed from the inside of the louvered vents, as shown in the photograph of Fig. 44. This appears to have increased the air flow and peak HRR slightly.

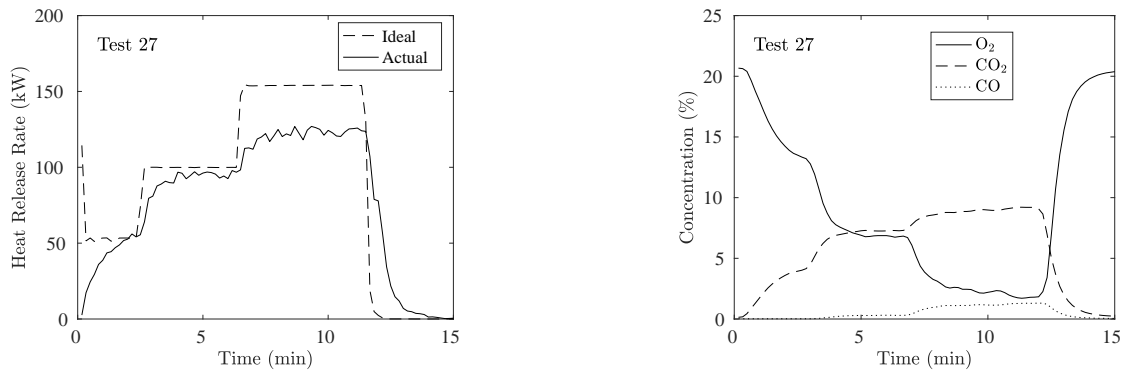
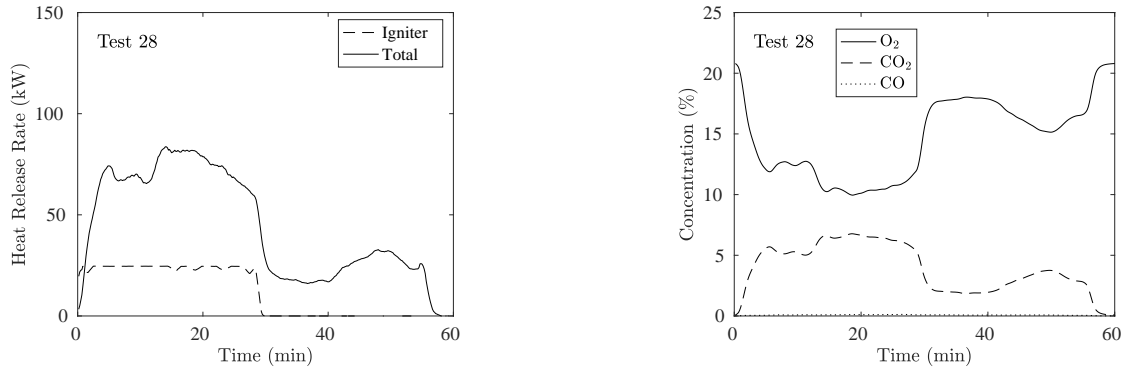


Fig. 44. Heat release rate, gas concentrations, and photograph of Experiment 27.

### C.28. Experiment 28

A tray of 5 kg of assorted plastics replaced the burner in Enclosure #4.



**Fig. 45.** Heat release rate, gas concentrations, and photograph of Experiment 28.

### C.29. Experiment 29

The 30 cm (1 ft) natural gas burner was positioned in the left rear of Enclosure #1. All vents were covered. A small view port was cut out of the front door panel and covered with quartz glass, as shown in Fig. 46.

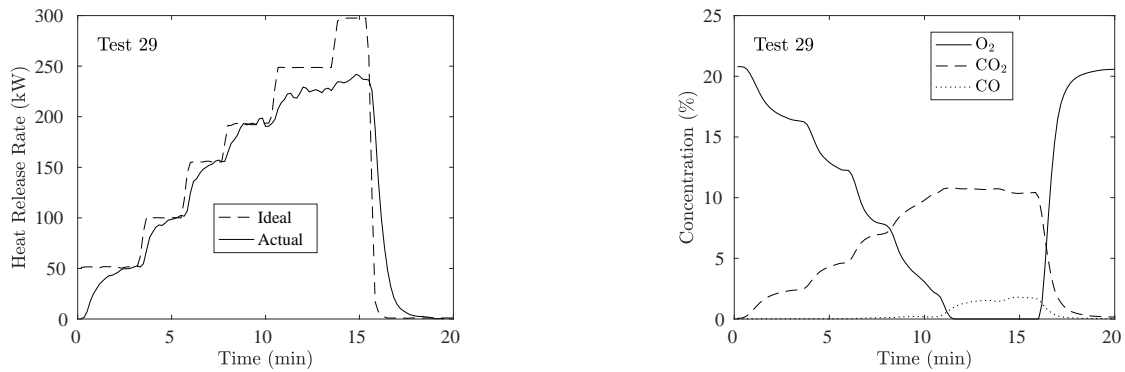


**Fig. 46.** Heat release rate, gas concentrations, and photograph of Experiment 29.

### C.30. Experiment 30

Experiment 30 was a repeat of Experiment 29, except that the lower right vent was uncovered as shown in the photograph of Fig. 47.

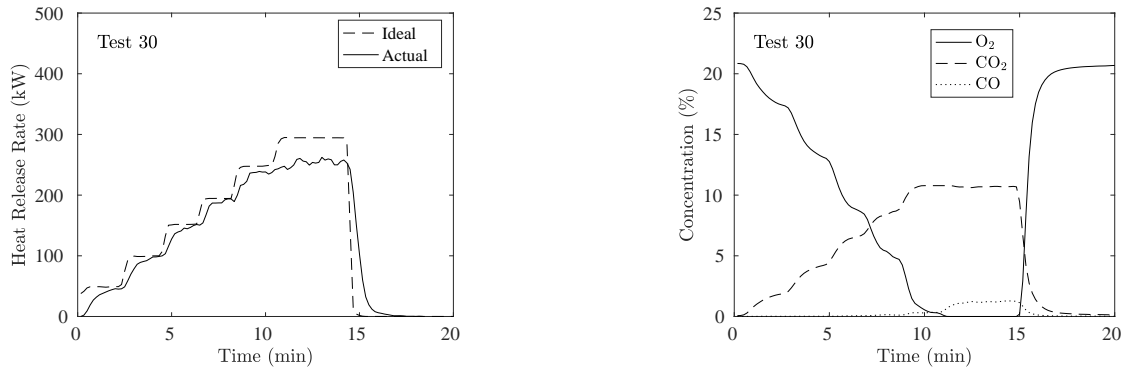


Fig. 47. Heat release rate, gas concentrations, and photograph of Experiment 30.

### C.31. Experiment 31

Experiment 31 was a repeat of Experiment 29, except that the upper right vent was uncovered as shown in the photograph of Fig. 48.

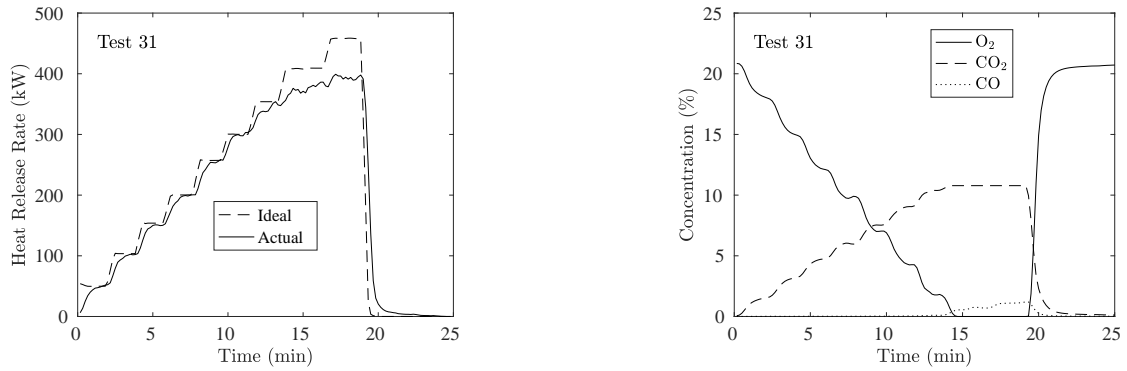


Fig. 48. Heat release rate, gas concentrations, and photograph of Experiment 31.

### C.32. Experiment 32

A tray of assorted plastics plus 30 cable segments used previously of length 3 m (10 ft) were hung within the left side of Enclosure #1. After the fire reached its peak HRR, water was applied to suppress the fire. After two attempts, the fire did not extinguish, at which point the rear door was opened and the fire spiked to 500 kW for approximately a minute as the unburned hydrocarbons trapped inside the enclosure were consumed. The fire's HRR decreased fairly quickly after this point. The photograph shown in Fig. 49 shows the black smoke billowing from the open door.

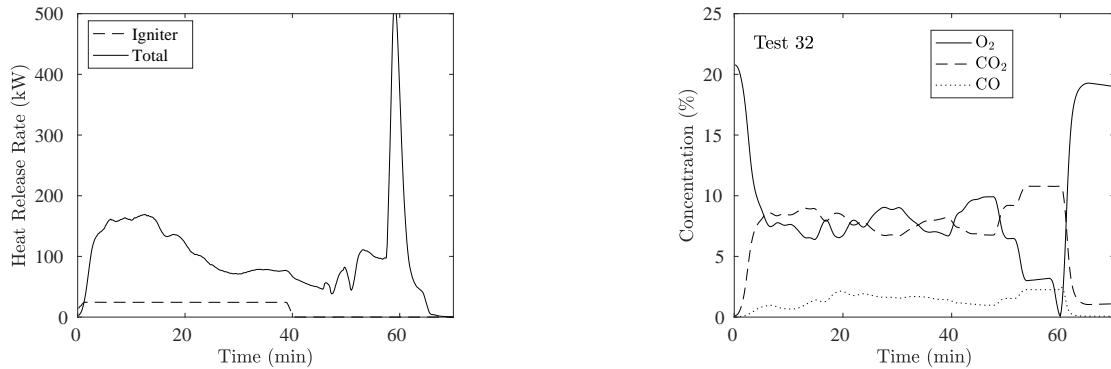


Fig. 49. Heat release rate, gas concentrations, and photograph of Experiment 32.